HHS Public Access

Author manuscript

Nat Protoc. Author manuscript; available in PMC 2024 September 17.

Published in final edited form as:

Nat Protoc. 2023 December ; 18(12): 3787–3820. doi:10.1038/s41596-023-00895-8.

Activation of mechanoluminescent nanotransducers by focused ultrasound enables light delivery to deep-seated tissue in vivo

Shan Jiang[1,2,4], **Xiang Wu**[1,2,4], **Fan Yang**[1,2,4], **Nicholas J Rommelfanger**[2,3], **Guosong Hong**[1,2,*]

[1]Department of Materials Science and Engineering, Stanford University, Stanford, CA, 94305, USA

[2]Wu Tsai Neurosciences Institute, Stanford University, Stanford, CA, 94305, USA

[3]Department of Applied Physics, Stanford University, Stanford, CA 94305, USA

[4]These authors contributed equally to this work.

Abstract

Light is utilized extensively in biological and medical research for optogenetic neuromodulation, fluorescence imaging, photoactivatable gene editing, as well as for light-based therapies. The major challenge to the implementation in vivo of light-based methods in deep-seated structures of the brain or of internal organs is the limited penetration of photons in biological tissue. The presence of light scattering and absorption have resulted in the development of invasive techniques such as the implantation of optical fibers, the insertion of endoscopes, and the surgical removal of overlying tissues, to overcome light attenuation and deliver it deep into the body. However, these procedures are highly invasive, and also make it difficult to reposition and adjust the illuminated area in each animal. Here, we detail a non-invasive approach to deliver light (termed deLight) in deep-tissue via systemically injected mechanoluminescent nanotransducers which can be gated using focused ultrasound. This approach achieves localized light emission with sub-millimeter resolution and millisecond response times in any vascularized organ of living mice without requiring invasive implantation of light-emitting devices. For example, deLight enables optogenetic neuromodulation in live mice without a craniotomy or brain implants. deLight provides a generalized method for applications that require a light source in deep tissues in vivo, such as deep-brain fluorescence imaging and photoactivatable genome editing. The implementation of the entire protocol for an *in vivo* application takes ~1-2 weeks.

[*]Corresponding author: guosongh@stanford.edu.

Author contributions

S.J., X.W., F.Y., N.J.R., and G.H. contributed ideas and designed research. S.J. and F.Y. synthesized MLNTs. S.J., X.W., F.Y., and N.J.R. characterized MLNTs in PDMS phantoms and artificial circulatory systems under FUS. S.J. and X.W. performed the application of deLight system for non-invasive sono-optogenetic neuromodulation in live mice. S.J., X.W., F.Y., N.J.R., and G.H. wrote the paper.

COMPETING INTERESTS

-In the interests of transparency and to help readers form their own judgements of potential bias, Nature Research journals require authors to declare any competing financial and/or non-financial interests in relation to the work described in the submitted manuscript. The corresponding author is responsible for submitting a competing interests statement on behalf of all authors of the paper. Please include the appropriate competing interests' statement. Either "No , I declare the authors have no competing interests as defined by Nature Research, or other interests that might be perceived to influence the interpretation of the article." or state full details of the competing interest See more details about our requirements here https://www.nature.com/authors/policies/competing.html

EDITORIAL SUMMARY

Non-invasive delivery of light in deep-tissue via focused ultrasound-activated and systemically injected mechanoluminescent nanotransducers to achieve localized light emission with sub-millimeter resolution and millisecond response times.

PROPOSED TWEET

With DeLight, focused ultrasound activates circulating mechanoluminescent nanotransducers as light sources in deep seated tissue

PROPOSED TEASER

mechanoluminescent nanotransducers as in vivo light source

Introduction

Many forms of energy have been used to interact with biological systems, such as light, electric fields, magnetic fields, and ultrasound waves.[1-6] Among them, light has widespread applications in bidirectional communication with living matters, such as imaging, neuromodulation and phototherapies.[7-9] However, one common challenge for these applications *in vivo* arises from the difficulty of efficiently delivering photons deep inside the body, as a result of severe attenuation of light by the highly scattering biological tissues.[9] Conventional approaches to address this challenge usually involve invasive implantation of external devices, such as optical fibers for optogenetics neuromodulation[10] and microendoscopes for neural activity imaging in the deep brain.[11,12] These implants induce acute tissue damage and chronic immune responses around the implantation site, which significantly alter the local physiological environment. As a result, current approaches for *in vivo* light delivery face the tradeoff between penetration depth and invasiveness, hampering their utility and capability in both research and clinical settings.

To address this challenge, several innovative methods for *in vivo* light delivery have been demonstrated. For example, implantable micro light emitting diodes (μ-LEDs) powered by radio frequency (RF) waves have been used as wireless light sources for deep-tissue optogenetics neuromodulation in both the central and peripheral nervous systems of freely moving animals.[13-15] This method replaces the physical connection between the animal and the external light source with free-space RF waves, thus effectively freeing the subject from tethering. However, the requirement for chronic implants still inevitably induces tissue damage. Additionally, upconversion nanoparticles (UCNPs), which convert tissue-penetrating near-infrared (NIR) light into visible light, have also been used as nanoscopic light sources for deep-brain optogenetics.[16] Although this method eliminates chronic tissue implants, the delivery of UCNPs into the brain still requires invasive brain surgeries. Furthermore, although NIR light is less scattered by biological tissues than visible light, its tissue penetration depth is still limited to a few millimeters before noticeable thermal effect is generated in the superficial tissue.[17] Therefore, although systemic delivery may represent a less invasive route for delivering UCNPs, their effectiveness is still constrained by the limited penetration depth of NIR light and the inability to confine the stimulation area

precisely. Furthermore, another method to overcome photon scattering inside the tissue is through wavefront shaping. Specifically, a spatial light modulator (SLM) was used to decode the wavefront change of an ultrasound guidestar and encode the reverse wavefront onto the incident light field, thus allowing tight focusing of 532-nm light to a spot of <30 μm at 2-mm depth inside acute brain slices.[18] The wavefront shaping method for deep-tissue light delivery does not require any implants and is thus non-invasive. However, the penetration depth of this method is limited only to a few millimeters by the efficiency of the ultrasound guidestar.

Despite these recent advances in deep-tissue light delivery methods, the tradeoff between tissue penetration depth and invasiveness remains largely unresolved. To address this challenge, we developed an ultrasound-mediated non-invasive **de**ep-tissue **light** source, named “deLight”, based on circulation-delivered mechanoluminescent nanotransducers (MLNTs).[19-24] Specifically, MLNTs are luminescent colloidal materials with engineered defects. The bandgap of MLNTs allows them to absorb ultraviolet light, which excites the electron in the valence band to the conduction band (process 1, Fig. 1a). The excited electron is then trapped by the defects, where the photoexcitation energy is stored without emission (process 2, Fig. 1a). Upon mechanical perturbation (e.g., ultrasound), the trapped electron is detrapped, returning to the conduction band (process 3, Fig. 1a). Then this electron undergoes a radiative relaxation process to transition to the valence band with concomitant light emission (process 4, Fig. 1a). Furthermore, these MLNTs can be systemically delivered into the circulatory system *in vivo*, generating localized light emission upon non-invasive stimulation of tissue-penetrant focused ultrasound (FUS, Fig. 1b). Comprehensive studies examining the biodistribution, excretion, and toxicology of MLNTs administered systemically in mice suggest that MLNTs exhibit excellent biocompatibility and minimal adverse effects.[22,23] We demonstrated that deLight can non-invasively activate channelrhodopsin-2 (ChR2)-expressing neurons in the mouse brain, producing significant changes in the behavior of the mouse and immunostained c-fos activity via a specific neurotechnology termed “sono-optogenetics”. Here we provide a comprehensive protocol for deLight, including the synthesis of the MLNTs with emission wavelengths covering the entire visible spectrum, optical characterizations of MLNTs in PDMS phantoms and artificial circulatory systems under FUS, and a specific demonstration of deLight for non-invasive optogenetics neuromodulation.

Development of the protocol

The deLight method takes advantage of tissue-penetrant FUS to gate light emission in deep tissue from circulating MLNTs, which can store the photoexcitation energy inside their crystal lattice and release it in the form of light upon localized mechanical stimuli.[19,20] We recently developed a biomineral-inspired suppressed dissolution approach to produce multi-color water-dispersible MLNTs from their micron-sized solid-state precursors.[22-24] The produced MLNTs form stable suspensions in aqueous solutions and can be repeatedly “charged” and “discharged” with continuous photoexcitation and FUS pulses, respectively.

To enable reproducible light emission upon FUS stimulation, deLight utilizes the endogenous circulatory system to implement the recharge and discharge cycles after the

systemic delivery of MLNTs. First, excitation light can be applied to superficial vessels near the skin to recharge circulating MLNTs therein. Second, charged MLNTs migrate to deep tissue via the continuous *in vivo* vascular network, emit light locally at the focus of ultrasound, and thus become discharged. Third, discharged MLNTs keep circulating inside the body and become recharged again when they return to superficial vessels under continuous photoexcitation. Therefore, the endogenous circulatory system is effectively turned into an "optical flow battery", enabling deep-tissue light emission at any location or depth on demand without any invasive implants or surgical removal of overlying tissues. We have validated the feasibility of deLight both in an *ex vivo* artificial circulatory system and in an *in vivo* mouse model. Additionally, we have also demonstrated the *in vivo* utility of deLight in a special application of non-invasive neuromodulation in the live mouse brain.

Applications of the protocol

The deLight method provides a versatile approach to non-invasively produce a light source deep inside the biological tissue, thus enabling any applications that require light *in vivo*. Specifically, a representative application of this protocol, as demonstrated in our recent works[19-22], is non-invasive optogenetic neuromodulation in live rodent brains. Using deLight to modulate opsin-expressing neurons *in vivo* enables the dissection of complex neural circuitry and potential treatment of neurological disorders, such as Parkinson's and Alzheimer's diseases. Apart from optogenetics, deLight can also be used to provide an excitation light source for deep-tissue fluorescence imaging, such as deep-brain calcium and voltage imaging through the intact scalp and skull.[23] Furthermore, deLight offers a non-invasive method to control other light-gated systems *in vivo*, such as photoactivatable CRISPR-Cas9 systems for genome modification and photosensitizers for cancer therapy in deep tissues.[25,26] We envision that the wide adoption of deLight will transform the field of biophotonics by significantly expanding the utilities of any biotechniques that require light *in vivo*.

Comparison with other methods

Compared with other deep-tissue light delivery methods, such as implanted light sources based on optical fibers or μ-LEDs, intracranially-injected light sources based on UCNPs, and wavefront shaping methods based on SLMs, the advantages of deLight are at least threefold. First, owing to the deep penetration of ultrasound in biological tissue, deLight can produce light emission inside the tissue at a depth >1 cm without the surgical removal of any overlying tissues (e.g. craniotomy) or invasive implantation of light sources. In contrast, both implanted and injected light sources inevitably cause tissue damage and immune responses around the surgical and implantation sites[27,28], while the penetration depth of UCNP- and SLM-based methods are usually restricted to a few millimeters[16,18]. Second, the light emission spot of deLight can be easily relocated throughout the body by simply scanning the focal spot of the ultrasound in all three dimensions. The ability to relocate the illuminated region is particularly challenging for implanted or injected light sources, which exhibit fixed illumination volumes near the site of implantation or injection. Third, deLight can access organs that are generally refractory to fiber implantation or invasive surgeries, such as the lung, heart, and gastrointestinal tract, owing to the absence of a physical implant *in vivo* to overcome structural and functional constraints.[29,30]

Expertise needed to implement the protocol

The synthesis of the MLNTs requires facilities such as a fume hood and special equipment such as a tube furnace, a centrifuge, and a ball-mill machine. The implementation of these synthesis procedures requires general wet laboratory training. The following procedures, such as optical and spectral characterizations of the MLNTs under FUS, require an optical table and a complete FUS system. Furthermore, *in vivo* mouse optogenetic studies require specific skills including retro-orbital injection, tail vein injection, transcardial perfusion, and immunohistochemistry staining. For researchers unfamiliar with these animal procedures, we recommend to practice by following online tutorials and attending hands-on workshops before attempting the deLight application. An animal husbandry facility is required for relevant optogenetic experiments in live rodents.

Limitations

Although deLight provides a new platform for deep-tissue light delivery in live animals, the relatively short lifetime (half-life up to 30 min) of systemically delivered MLNTs represents a potential constraint for *in vivo* applications over longer time. To mitigate this challenge, additional administrations of MLNTs are required if a consistent light source with duration longer than 30 min is needed. Furthermore, at the current stage, the need for an ultrasound transducer to deliver ultrasound stimuli *in vivo* requires head fixation of animals. However, we envision that the engineering of a wearable ultrasound transducer will enable deLight in freely moving animals.[31] Moreover, since the application of ultrasound may cause non-specific activation of the peripheral auditory pathway,[32-34] experiments must be carefully designed to rule out potential confounding effects besides FUS-produced light emission. Specifically, when deLight is used for sono-optogenetic neuromodulation, it is recommended that the applied ultrasound waves be smoothed out to remove any undesirable auditory responses in the mouse brain.[35] Additionally, when deLight is used for sono-optogenetics, FUS alone may activate the widely expressed mechanoreceptors inside the brain, thus masking the effect of light emission in the specific activation of opsin-expressing neurons. Therefore, restricting the ultrasound intensity below the threshold intensities that have been reported to stimulate neurons by FUS alone at certain frequencies[36] will ensure the desirable effect of neuromodulation by deLight. Lastly, although the current deLight protocol disallows concurrent fluorescent imaging with FUS stimulation, simultaneous calcium or voltage imaging of deLight-stimulated brain regions can be achieved with advanced engineering in both FUS transducer and the imaging system.[37]

Experimental design

In this protocol, we include detailed procedures for producing MLNTs with their emission wavelengths covering the entire visible spectrum (Procedure 1). In addition, we also include detailed procedures for characterizing the ultrasound responses of MLNTs in tissue-mimicking phantoms (Procedure 2) and artificial circulatory systems (Procedure 3). Procedures 2 and 3 are required for examining the optical and spectral properties of the as-synthesized MLNTs for the implementation of deLight *in vivo*. Furthermore, we include a representative demonstration of deLight in two assays: a mouse behavioral assay and an

immunohistochemical assay of c-fos (Procedure 4). Researchers can choose from these two assays based on their specific experimental design.

Subjects

This protocol primarily describes the use of deLight to activate ChR2-expressing neurons in B6.Cg-Tg(Thy1-COP4/EYFP)18Gfng/J (Thy1-ChR2-YFP) mice of both sexes (6~12 weeks).[38] Additionally, researchers can choose from the four MLNTs introduced in this protocol for optogenetic neuromodulation with other wavelengths of visible light, such as activation of halorhodopsin for neural inhibition and red-shifted channelrhodopsin (ReaChR) for neural activation.

Controls

Proper controls are crucial in optogenetic studies. When using deLight for non-invasive optogenetics, we recommend the following control groups wherever the procedure permits: 1) Wild-type C57Bl/6J mice, which are recommended by the Jackson Laboratory as the proper control on the same genetic background for Thy1-ChR2-YFP mice, should be systemically delivered with MLNTs and stimulated with the same FUS protocol in the same brain region. 2) The same Thy1-ChR2-YFP mice systemically injected with 1x PBS carrier (sham injection) and stimulated with the same FUS protocol. This control can help rule out the possibility of nonspecific and direct neural activation with FUS via the activation of the auditory pathway or endogenous temperature-sensitive and mechanosensitive ion channels. This control becomes more crucial when using deLight on target organs and tissues outside the brain, considering the numerous mechanoreceptors (e.g., Piezo1 and TRPA1) found in these tissues.[39,40] 3) The same Thy1-ChR2-YFP mice, systemically delivered with MLNTs but without FUS stimulation, should be used as another control to help account for potential confounds caused by circulating MLNTs. 4) An internal control can be achieved by analyzing neural activity in the non-FUS-stimulated hemisphere of the same Thy1-ChR2-YFP mouse brain.

Regulatory Approvals—All procedures involving living animals must be approved by the Institutional Animal Care and Use Committee (IACUC) and comply with national guidelines regarding the use of animals in research. All procedures performed on mice here were approved by Stanford University's Administrative Panel on Laboratory Animal Care (APLAC). The time required to obtain permissions varies between months to one year, depending on the local committee. Institutional Material Transfer Agreements (MTAs) are also required if other research labs requested MLNTs from our lab. The submission for APLAC's approval and the establishment of MTAs represent straightforward and standard procedures that are inherent to the research process. Importantly, these steps do not necessitate any supplementary financial expenditures.

Materials

Biological materials

- Mice. Vertebrate animal subjects used in this protocol were Thy1-ChR2-YFP mice (The Jackson Laboratory, cat. no. 007612) and C57BL/6J mice (The

Jackson Laboratory, cat. no. 000664). All the animal procedures comply with the '3Rs' measures for the replacement, refinement and reduction of animals in research (Directive 2010/63/EU) and with the severity level of 1.

Reagents

- Strontium carbonate ($SrCO_3$; Sigma Aldrich, cat. no. 472018)
- Silicon dioxide (SiO_2; Sigma Aldrich, cat. no. 637238)
- Magnesium carbonate hydroxide pentahydrate ($(MgCO_3)_4{\cdot}Mg(OH)_2{\cdot}5H_2O$; Sigma Aldrich, cat. no. M5671)
- Europium(III) oxide (Eu_2O_3; Sigma Aldrich, cat. no. 323543)
- Dysprosium(III) oxide (Dy_2O_3; Sigma Aldrich, cat. no. 203181)
- Boric acid (H_3BO_3; Sigma Aldrich, cat. no.B7660)
- Copper(II) acetylacetonate ($Cu(C_5H_7O_2)_2$; Sigma Aldrich, cat. no. 514365)
- Chloroform (Fisher Chemical, AA32614K2)
- Zinc sulfide (ZnS; Sigma Aldrich, cat. no. 244627)
- Aluminum oxide (Al_2O_3; Sigma Aldrich, cat. no. 267740)
- Manganese(II) carbonate ($MnCO_3$; Sigma Aldrich, cat. no. 377449)
- Calcium carbonate ($CaCO_3$; Sigma Aldrich, cat. no. C4830)
- Titanium(IV) oxide, anatase (TiO_2; Sigma Aldrich, cat. no.637254)
- Praseodymium(III) oxide (Pr_2O_3; Thermo Fisher Scientific, cat. no. AA3566309)
- Compressed gas of 5% H_2 and 95% Ar (Linde Gas & Equipment Inc., cat. no. UN1954)
- Silicone oil (Thermo Fisher Scientific, cat. no. S159-500)
- Milli-Q water
- Sodium chloride (Thermo Fisher Scientific, cat. no. S271-50)
- Sodium citrate, 0.5M buffer soln. (Thermo Fisher Scientific, cat. no. AAJ61815AP)
- Sodium hydroxide (Thermo Fisher Scientific, cat. no. 7470-32)
- N,N-dimethylformamide (DMF; Thermo Fisher Scientific, cat. no. D119-1)
- Methoxy(polyethylene glycol)-silane, 20 kDa (mPEG-silane; Jenkem Technology, cat. no. A3100-1/M-SLN-20K)
- Polydimethylsiloxane (PDMS; Dow Corning, Sylgard 184)
- Ketamine (Dechra)
- Dexdomitor (Dechra)

- Antisedan (Zoetis, cat. no. 032800)
- Paraformaldehyde (PFA; Thermo Fisher Scientific, cat. no. AA433689M)
- 1x PBS (Thermo Fisher Scientific, cat. no.10010023)
- Ethanol, anhydrous (Thermo Fisher Scientific, cat. no. A405P-4)
- Sodium Phosphate Dibasic Anhydrous (Na_2HPO_4; Thermo Fisher Scientific, cat. no. S374-500)
- Sodium Phosphate Monobasic Monohydrate ($NaH_2PO_4 \cdot H_2O$; Thermo Fisher Scientific, cat. no. S369-500)
- Sucrose (Thermo Fisher Scientific, cat. no. S5-500)
- O.C.T. compound (Optimal cutting temperature compound, Sakura Finetek USA, cat. no. 4583)
- Dry ice
- Methanol (Thermo Fisher Scientific, cat. no. A412P-4)
- Triton X-100 (Sigma Aldrich, cat. no.T8787)
- Normal donkey serum (Jackson ImmunoResearch Inc, cat. no. 017-000-121)
- Primary antibody (Table 2)
- Secondary antibody (Table 2)
- Mounting medium (Thermo Fisher Scientific, cat. no.P36931)

Equipment

- Agate mortar and pestle (Inner Diameter 150 mm, inner Depth 40 mm; Alpha Nanotech, cat. no. B07MPBJ2WX)
- Balance (METTLER TOLEDO, cat. no. XSR105)
- Weighing paper (Thermo Fisher Scientific, cat. no. 09-898-12A)
- Spatula (Sigma Aldrich, cat. no. Z560049)
- Tube furnace (CarboliteGero, cat. no. TF1 16/60/180)
- Alumina crucible (AdValue Technology, cat. no. AL-1005)
- Combustion boat (AdValue Technology, cat. no. AL-3060)
- X-ray diffractometer (Malvern Panalytical, PANalytical Empyrean)
- 1~20 ml glass vial (Thermo Fisher Scientific)
- Ball-mill machine (SPEX SamplePrep, cat. no. 8000D Dual Mixer/Mill)
- Tungsten Carbide Grinding Vial Set (SPEX SamplePrep, cat. no. 8004)
- Sand (Thermo Fisher Scientific, cat. no. MSX00761)
- Temperature controller (J-Kem Scientific, cat. no. 210/TIMER-J-S)

- Single neck round bottom flask, 14/20 outer joint (Chemglass Life Sciences, cat. no. CG-1506-94)
- Condenser
- Rubber plug (Thermo Fisher Scientific)
- Hot plate stirrer (Thermo Fisher Scientific, cat. no. SP88857290)
- Dialysis tubing (Spectra/Por®, cat.no. Spectra Standard RC Trial Kit MWCO:30 kD)
- Glass rod (Thermo Fisher Scientific)
- Pyrex beaker (Thermo Fisher Scientific, cat. no. 50-121-5006)
- Transmission electron microscope (TEM) (FEI Company, FEI Tecnai TEM)
- Crystallizing dish (PYREX, cat. no. 3140-170)
- Centrifuge tubes (Corning, cat. no. 430290)
- Centrifuge (Thermo Fisher Scientific, cat. no.75004220)
- Sonicator (Cole-Parmer, cat. no.EW-08895-59)
- Milli-Q Advantage A10 water purification system (Sigma Aldrich, cat. no. Z00Q0V0WW)
- UV-Vis spectrophotometer (Thermo Fisher Scientific, cat. no. 840-310800)
- ICP-MS (Thermo Fisher Scientific, Thermo Scientific, cat. no. XSERIES 2 ICP-MS)
- Vacuum desiccator (Bel-Art Products, cat. no. F42025-0000)
- Glass petri dish (VWR, cat. no. 89000-280)
- Oven (Thermo Fisher Scientific, cat. no. 51028115)
- FUS (Image Guided Therapeutics)
- Ultrasound gel (Aquasonic, cat. no. 100)
- Needle hydrophone (Precision acoustics, cat. no. NH0200)
- DC coupler (Precision acoustics, cat. no. DCPS)
- Oscilloscope (Keysight, cat. no. MSOX2024A)
- 50 Ω impedance adapter (Rigol, cat. no. ADP0150BNC)
- 2.5 l crystallizing dish (PYREX, cat. no. 3140-90)
- UV light emitting diode lamp (UV-LED lamp; Thorlabs, cat. no. SOLIS-365C)
- Optical power meter (Thorlabs, cat. no. PM200)
- Optical table
- Spectrometer (Ocean Insight, cat. no. OCEAN-HDX-VIS-NIR)

- Optical fiber (Ocean Insight, cat. no. QP600-1-UV-VIS)
- Collimating Lens (Ocean Insight, cat. no. 74-ACR)
- Thorlabs camera (Thorlabs, cat. no. CS165MU)
- Camera lens (Schneider Kreuznach, cat. no. ONYX 0.95/25 C)
- Multifunction I/O Device (National Instruments, cat. no. USB-6221)
- BNC cables
- Tygon tubing (Mcmaster Carr, cat. no. 5155T12)
- Peristaltic pump (Instech, cat. no. P720)
- UV-LED (Thorlabs, cat. no. M365LP1)
- DC power supply (Eventek, cat. no. KPS305D)
- 3D printed holder
- Thorlabs camera (Thorlabs, cat. no. CS165MU)
- Camera lens (Schneider Kreuznach, cat. no. ONYX 0.95/25 C)
- Ultra thin magnetic stirrer (Thermo Fisher Scientific, cat. no. 14-955-149)
- Stir bar
- Flask clamp
- Black aluminum foil
- Photodiode (Thorlabs, cat. no. SM05PD1A)
- Photodiode amplifier (Thorlabs, cat. no. PDA200c)
- Heating pad (Harvard Apparatus, cat. no. 55-7020)
- Surgical tools (Fine science tools, cat. no. 11023-10: tissue forceps; cat. no. 11000-12: standard pattern forceps; cat. no. 14060-09: fine scissors, sharp)
- Hair removal lotion (Nair, Church & Dwight)
- Video recording device (Canon, cat. no. VIXIA HF W11)
- Timer
- 29 gauge insulin syringe (Thermo Fisher Scientific, cat. no. 14-841-33)
- Perfusion pump (Harvard Apparatus, cat. no. 70-4504)
- Needle (27 gauge)
- Syringe (0.5 - 20 ml)
- Tissue adhesive (3M, cat. no. 1469SB)
- Eye ointment (Genteal, cat. no. B000URVDQ8)
- UV flashlight (Consciot, cat. no. ACE002-US)

- Water absorbing pad
- Brain slicer (Zivic. Instruments, cat. no. 5325)
- Razor blade (LORD International, cat. no. B0047M56BA)
- Kimwipes (Kimtech Science™, cat. no. 34120)
- Tissue embedding mold (Thermo Fisher Scientific, cat. no. NC9542860)
- Cryostat (Leica, cat. no. CM3050)
- Microtome blades (Thermo Fisher Scientific, cat. no. 3150734)
- 10 - 1000 µl pipette tip (Thermo Fisher Scientific)
- 10 - 1000 µl mechanical pipette (Eppendorf)
- 48-well plate (Corning, cat. no. 3548)
- Parafilm (Bemis, cat. no. PM996)
- Microplate shaker (Thermo Fisher Scientific, cat. no. 88-861-023)
- 4 degree fridge
- Aluminum foil (Thermo Fisher Scientific, cat. no. 01-213-100)
- Paintbrush (Princeton Brush Company, Series 9100 (5/0))
- Superfrost™ plus glass slides (Fisher Scientific, cat. no. 22-037-246)
- Coverslips
- Nail polish
- Confocal microscope (ZEISS, LSM 980 with Airyscan 2)

Reagent setup

Copper stock solution—Prepare a solution of 0.01 mol/l copper acetylacetonate in chloroform. May store at room temperature (25 °C) indefinitely.

Sodium citrate buffer—Prepare a solution of 0.08 mol/l sodium citrate in Milli-Q water. May store at room temperature indefinitely.

Anesthetic drugs—Prepare the anesthetic drug (16 mg/ml Ketamine and 0.2 mg/ml Dexdomitor) by mixing 0.8 ml of stock Ketamine solution, 2 ml of stock Destomitor solution, and 2.2 ml of 1 **X** PBS. Store at room temperature for up to 1 month.

70% ethanol—Dilute anhydrous ethanol in Milli-Q water. Store at room temperature for up to a month.

Antisedan drug—Prepare the antisedan drug (0.5 mg/ml) by diluting the stock antisedan drug (5 mg/ml) 10 times in 1x PBS. Store at room temperature for up to a month.

PFA solution (4% (wt/vol))—Prepare the PFA solution (4% (wt/vol)) by diluting the stock PFA solution (16% (wt/vol)) with 1 **x** PBS. PFA solution should be prepared fresh before use.

CAUTION PFA is toxic if inhaled, swallowed, or in contact with the skin, causing severe skin and eye damage. May cause cancer. Handle with care under a fume hood and wear appropriate personal protective equipment (PPE) (e.g., gloves, mask, and laboratory coat).

Na_2HPO_4 stock solution—Prepare a solution of 28.4 g/l Na_2HPO_4 in Milli-Q water. May store at room temperature indefinitely.

NaH_2PO_4 stock solution—Prepare a solution of 24.2 g/l NaH_2PO_4 in Milli-Q water. May store at room temperature indefinitely.

0.1 M Phosphate Buffer (PB)—For making 200 ml of PB solution, mix 81 ml of Na_2HPO_4 stock solution with 19 ml of NaH_2PO_4 stock solution. Then dilute to a total volume of 200 ml using Milli-Q water.

Sucrose solution—Prepare a solution of 30% (wt/vol) sucrose in 0.1 M PB solution. Store at room temperature for up to 1 month.

PBS Triton-X100—Prepare a solution of 0.3% (wt/vol) Triton-X100 in 1x PBS. May store at room temperature indefinitely.

Blocking buffer—Prepare a solution of 5% (vol/vol) normal donkey serum in 1x PBS Triton-X100 solution. Blocking buffer should be prepared fresh before use.

Washing solution—Prepare a solution of 0.05% (vol/vol) Triton-X100 in 1x PBS. May store at room temperature indefinitely.

Primary antibody solution—Dilute the primary antibodies in the blocking solution with an appropriate ratio (Table 2). The primary antibody solution should be prepared fresh before use.

Secondary antibody solution—Dilute the secondary antibodies with an appropriate ratio (Table 2) in 1x PBS with 5% normal donkey serum and 0.1% TritonX-100. The secondary antibody solution should be prepared fresh before use.

CAUTION Secondary antibodies are light-sensitive. Cover with aluminum foil after dilution.

Equipment setup

Tube furnace—Reference the user manual for programming the temperature control. https://www.carbolite-gero.com/products/control-options/epc3016p1/

Ball-mill machine—Seek expert guidance from the facility manager regarding the use of this equipment. General guidelines for setting up the ball-mill machine can be found in the following link: 8000d dual mixer/mill

The duration of a single session of the ball-milling process here is 10 min.

Camera—The operation of the camera in this protocol requires the installation of the software ThorCam.

General information regarding the software ThorCam can be found in the following link: https://www.thorlabs.com/software_pages/ViewSoftwarePage.cfm?Code=ThorCam

FUS system—The operation of the FUS system is customized by Image Guided Therapeutics. FUS transducers with center frequencies of 0.65-3.5 MHz have been demonstrated to produce intense emission from MLNTs described in this protocol. The representative transducer used in the protocol is a 1.5 MHz transducer with a diameter of 38.2 mm, a weight of 40 g, and a lateral focal spot size of 1.0 mm. The maximum power supplied to the transducer used in this protocol is 50 W. In addition, the actual input power can be determined as the product of the drive amplitude (in percentage) and the maximum input power (50 W). The operation of the FUS system requires the installation of the software BBBop. Contact the vendor for further information.

https://www.igtradiology.com/services/ultrasound/

Ocean optics spectrophotometer—The operation of the ocean optics spectrophotometer in this protocol requires the installation of the software OceanView. General information regarding the software OceanView can be found in the following link: https://www.oceaninsight.com/globalassets/catalog-blocks-and-images/manuals--instruction-ocean-optics/software/oceanviewio.pdf

Perfusion pump—Select the syringe volume of the perfusion syringes used in the procedure and set the flow rate to 5 ml/min.

Cryostat—General information regarding the operation of the cryostat can be found in the following link: https://www.leicabiosystems.com/us/histology-equipment/cryostats/leica-cm3050-s/

In this protocol, the temperature of the operation chamber was set to −20 °C, the blade temperature was set to −18 °C, and the sectioning thickness was set to 40 μm.

Microscope—Seek expert guidance from your local imaging facility to set up the microscope. General guidelines for the ZEISS LSM 980 with Airyscan 2 can be found in the following link: https://www.zeiss.com/microscopy/en/products/light-microscopes/confocal-microscopes/lsm-980-with-airyscan-2.html

Software

LabVIEW—LabVIEW software is required for acquiring the optical power measurements of the mechanoluminescent emission from the artificial circulatory system. General information regarding LabVIEW can be found in the following link: https://www.ni.com/en-us/support/downloads/software-products/download.labview.html#477380

Matlab—For synchronizing the control of the FUS transducer, the UV-LED, and the camera, the installation of the software Matlab is required in this protocol. General information on Matlab can be found in the following link: https://www.mathworks.com/products/matlab.html

ImageJ—For analyzing the line profile of the mechanoluminescence emission and the confocal imaging of the stained brain slices, the installation of the software ImageJ is used in this protocol. General information on ImageJ can be found in the following link: https://imagej.net/software/fiji/

Procedure 1 Synthesis of MLNTs

Synthesis of bulk mechanoluminescent materials via solid-state reactions Timing 2 d

CRITICAL The detailed reagent compositions for producing each bulk mechanoluminescent material are listed in Table 1.

1. Prepare all reagents needed for synthesis.
2. Weigh all reagents using a balance and transfer all reagents to an agate mortar.
3. Grind the reagents using an agate pestle for 1 h (Fig. 2a).
4. Transfer the ground reagents into an alumina crucible (Fig. 2b) and place the crucible on an alumina combustion boat.

   CRITICAL STEP Do not use porcelain crucibles and combustion boats since both can only be used under 1050 °C. In contrast, alumina crucibles and combustion boats can withstand temperatures up to 1750 °C.
5. Place the combustion boat into the tube furnace (Fig. 2c) with a hook carefully (Fig. 2d) and make sure the combustion boat is right in the heating zone of the tube furnace. Tightly seal the end, which has the tubing connected to the gas cylinder. Connect the other end of the furnace with another tubing and immerse the open end of the tubing in a beaker filled with water inside the fume hood.
6. (Optional) Turn on the gas cylinder containing 5% H_2 in Ar and make sure the gas flow is stable.

   CRITICAL STEP Only $Sr_2MgSi_2O_7$:Eu,Dy, ZnS:Cu,Al, and ZnS:Mn require 5% H_2 in Ar during synthesis. $CaTiO_3$:Pr needs to be synthesized in air. When gas flow is needed, the open end of the tubing is placed inside a water-containing beaker for monitoring the gas flow rate via the production of gas bubbles.

7. Run the pre-set program of the furnace. After the program is complete, let the furnace cool down to room temperature.

   CRITICAL STEP The detailed temperature settings for producing each bulk mechanoluminescent material are listed in Table 1.

8. (Optional) Turn off the gas when the program is finished.

9. After the furnace is cooled down to room temperature, take out the combustion boat from the furnace with the hook carefully.

   CAUTION Hot surfaces! Make sure the furnace has cooled down to room temperature.

10. Transfer the as-synthesized bulk mechanoluminescent materials out of the crucible into the agate mortar and roughly grind the materials with a pestle for 1 min.

11. Collect the as-prepared mechanoluminescent materials into a glass vial.

    CRITICAL Examine the color of the as-synthesized materials under room light and their afterglows in the dark. Each material should exhibit the afterglow as shown in Fig. 3.

    TROUBLESHOOTING

12. Measure X-ray diffraction (XRD) patterns of as-prepared mechanoluminescent materials. Ensure their XRD patterns match the standard JCPDS cards ($Sr_2MgSi_2O_7$: 75-1736, ZnS: 79-2204, and $CaTiO_3$: 42-0423).

    PAUSE POINT The materials can be stored in air at room temperature for over one year.

13. Load a tungsten carbide grinding vial with the materials from Step 11 and one 7/16 in. (11.2 mm) tungsten carbide ball (Fig. 4a).

14. Seal the vial with a screw-on tungsten carbide-lined cap and place it in a clamp of the ball-mill equipment (Fig. 4b).

15. Tighten the clamp with the knob, and lock the clamp with the locking tab. Close the lid of the ball-mill machine and fasten it with the manual latch.

    CRITICAL STEP When mounting the grinding vials in the ball-mill equipment, note that two clamps must be balanced with a load. If only one sample is loaded, place an empty vial in the other clamp.

16. Start the ball-milling process with three 10-min sessions and a 5-min interval between sessions.

17. Take the vial out of the clamp and collect the ball-milled material.

    CRITICAL STEP Usually there will be a residue of ball-milled materials stuck to the grinding vial and the grinding ball. To remove this residue and clean the grinding setup, pour a small amount of sand into the grinding vial and start a ball-milling process for 10 min.

PAUSE POINT The ball-milled materials can be stored at room temperature for over a year.

Synthesis of MLNTs via a biomineral-inspired suppressed dissolution approach Timing 3 d

18. Load the flask with 2 g of the material in Step 17 and 240 ml of the sodium citrate buffer (0.08 mol/l).

19. Set the oil bath to 80 °C.

20. Immerse the flask in the oil bath and connect a condenser to the flask (Fig. 4c).

CRITICAL STEP Make sure the level of the oil is higher than that of the solution inside the flask.

CAUTION Hot surfaces! Handle with care.

21. Turn on the magnetic stirrer and start a timer for 72 h for the suppressed dissolution process.

PAUSE POINT The as-etched materials can be stored at room temperature for over a year.

Surface modification of biocompatible MLNTs Timing 2 d

22. After the suppressed dissolution process, transfer all materials from their original container (i.e., the reaction flask or storage container) to centrifuge tubes.

23. Start the centrifugation process at 1000 rpm (116 rcf) for 10 min and collect the supernatant containing colloidal MLNTs (Fig. 4d).

24. Transfer the colloidal solution into a beaker and add sodium chloride (3 g / 10 ml) to the solution to facilitate the collection of the colloid at a relatively low centrifugation speed for its purification.

25. Stir the colloidal solution with a glass rod to facilitate the dissolution process of sodium chloride and wait for 30 min (Fig. 4e).

26. Transfer the solution from Step 25 into centrifuge tubes and start the centrifugation process at 5000 rpm (2907 rcf) for 10 min.

CRITICAL STEP Avoid using high centrifugation speed over 5000 rpm (2907 rcf), which may cause irreversible agglomeration of MLNTs during surface modification.

27. Remove the supernatant from all centrifuge tubes.

28. Disperse the pellets in Milli-Q water to a total volume of 5 ml.

29. Transfer the colloidal solution from Step 28 into a clamped cellulose dialysis tubing with a molecular weight cutoff of 30 kDa.

30. Hang the dialysis tubing on a glass rod via a rubber band and place the glass rod on top of a 2 l glass beaker containing Milli-Q water (Fig. 4f).

31. Turn on the magnetic stirrer and dialyze for 48 h to remove excess ions, such as citrate, Na^+, Cl^-, and etched ions, from the colloidal solution. The presence of these ions may interfere with the following measurements for determining the concentration of MLNTs.

CRITICAL STEP Change the bath with fresh Milli-Q water with a total of six water changes during dialysis.

32. Collect the colloidal solution from the dialysis bag in a glass vial.

33. Acquire TEM images of colloidal MLNTs after dialysis to make sure that the diameters of MLNTs are in the range of 10~110 nm. Representative TEM images of colloidal MLNTs composed of $Sr_2MgSi_2O_7$:Eu,Dy, ZnS:Cu,Al, ZnS:Mn, and $CaTiO_3$:Pr can be found in Extended Data Fig. 1.

34. Dilute the solution prepared in Step 32 into three different concentrations and measure their corresponding UV-Vis spectra over a wavelength range from 400 nm to 700 nm with a UV-Vis spectrophotometer.

CRITICAL STEP We recommend making 100x, 200x, and 300x dilutions of the solution from Step 32. Make sure the measured absorbance values are below 1 for an optical path length of 1 cm in the entire spectral range of measurements.

35. Measure the mass concentrations of the solutions tested in Step 34 via inductively coupled plasma mass spectrometry (ICP-MS).

36. Determine the extinction coefficient ε of the colloidal solution per mg of the colloid per ml (ml mg^{-1} cm^{-1}) via linear fitting of the measured absorbance at 400 nm at three concentrations (from Step 34) vs their mass concentrations determined by ICP-MS (from Step 35) for each MLNT material.

CRITICAL STEP The concentration of each colloid is calculated based on the Beer-Lambert law ($A = \varepsilon lc$), in which A is the absorbance, ε is the extinction coefficient per mg of the colloid per ml (ml mg^{-1} cm^{-1}), l is the optical path length (cm), and c is the concentration (mg/ml) of the colloid.

37. Transfer 20 ml of the colloidal solution diluted to a concentration of 6 mg/ml from Step 32 into a glass vial and add 40 μl of sodium hydroxide solution (10 M).

TROUBLESHOOTING

38. Mount the glass vial with a flask clamp and immerse the glass vial into a water-filled sonicator for 1 h of sonication at room temperature (Fig. 4g).

39. Remove the glass vial from the clamp and transfer the solution into a centrifuge tube. Wash the colloids with Milli-Q water three times via a centrifugation-resuspension process. The centrifuge is set to 4000 rpm (1860 rcf) for 10 min, and the supernatant is removed after each wash before resuspending the pellet into 20 ml of Milli-Q water.

40. Wash the colloid with anhydrous DMF three times via a centrifugation-resuspension process. The centrifuge is set to 4000 rpm (1860 rcf) for 10 min, and the supernatant is removed after each wash before resuspending the pellet into 20 ml of DMF.

41. Disperse the colloid from the last wash into 10 ml of anhydrous DMF with sonication.

42. Transfer the suspended solution into a glass vial.

43. Add 40 mg of mPEG-silane (20 kDa) to the colloid in DMF.

44. Mount the glass vial with a flask clamp and immerse the glass vial into a water-filled sonicator for 4 h of sonication at 50 °C.

TROUBLESHOOTING

45. Remove the glass vial from the clamp and transfer the solution into a centrifuge tube.

46. Wash the colloids with anhydrous DMF three times via a centrifugation-resuspension process. The centrifuge is set to 4000 rpm (1860 rcf) for 10 min, and the supernatant solution is removed after each wash before resuspending the pellet into 20 ml of DMF.

47. Wash the colloid with Milli-Q water three times via a centrifugation-resuspension process. The centrifuge is set to 4000 rpm (1860 rcf) for 10 min, and the supernatant solution is removed after each wash before resuspending the pellet into 20 ml of Milli-Q water.

48. Disperse the PEGylated MLNTs from the previous step in 1 ml of Milli-Q water and transfer it to a glass vial.

    CRITICAL STEP Examine the color of each colloidal solution of MLNTs under room light and its afterglow in the dark. Each MLNT colloid should exhibit the afterglow of its corresponding color as shown in Fig. 4h-k in the dark. When examining the color of the MLNT colloidal solutions, note that the afterglow intensity naturally decays without further charging. Specifically, it takes ~3 min to thermally dissipate all stored energy in MLNTs of $Sr_2MgSi_2O_7$:Eu,Dy to 1%. All four MLNTs are ranked in terms of their power and energy storage capability as follows: $Sr_2MgSi_2O_7$:Eu,Dy > ZnS:Cu,Al > ZnS:Mn > $CaTiO_3$:Pr.

    TROUBLESHOOTING

    PAUSE POINT The PEGylated MLNTs can be stored at room temperature for up to a week.

Procedure 2 Characterizations of MLNTs in a tissue-mimicking phantom

Preparation of the tissue-mimicking phantom uniformly doped with MLNTs Timing 1 h

1. Dry MLNTs prepared from Step 32 in Procedure 1 in air and grind them roughly with an agate mortar and a pestle.

2. Prepare 1.54 g of PDMS base, 0.15 g of PDMS curing agent, and 112 mg of dried MLNTs.
3. Add the PDMS base, PDMS curing agent, and MLNTs into a glass petri dish.
4. Mix all the materials until the MLNTs are uniformly distributed in the mixture.
5. Place the glass petri dish in a vacuum desiccator and vacuum for 30 min to remove air bubbles.
6. Remove the glass petri dish from the vacuum desiccator and place it in a 70 °C oven for 30 min.

   CAUTION Hot glass petri dish. Handle with care.
7. After the PDMS phantom is cured, remove the petri dish from the oven and separate the phantom from the glass petri dish.

   PAUSE The phantom may be stored at room temperature indefinitely.

   TROUBLESHOOTING

(Optional) Calibration of FUS transducers with a needle hydrophone Timing 1 d

CRITICAL The calibration of a FUS transducer, which entails the derivation of the relationship between the drive amplitude and ultrasound peak pressure, is required for every new FUS transducer before use. Fig. 5a shows a schematic illustration of the calibration setup described in Steps 8-12.

8. Connect the FUS system to a computer with a USB-to-USB-Type-B cable.
9. Connect the needle hydrophone to the DC coupler.
10. Connect the DC coupler to an oscilloscope with a BNC-to-BNC cable and a 50-Ω impedance adapter.

    CRITICAL STEP If the oscilloscope has an input impedance of 50 Ω, then the 50-Ω impedance adapter is not needed in this step.
11. Mount the FUS transducer on a stereotaxic manipulator.
12. Immerse the FUS transducer and the needle hydrophone into a water-filled 2.5 l glass tank (Fig. 5b). Align the transducer plane perpendicular to the axis of the needle hydrophone (Fig. 5c).

    CRITICAL STEP Aligning the transducer and the needle hydrophone is crucial for the calibration. If the axis of the needle hydrophone is not perpendicular to the transducer plane, the calibration results will not be accurate.
13. Turn on FUS hardware and open the BBBop software.
14. Set the FUS pulse amplitude to 5%, pulse duration to 200 ms, and delay to 800 ms.
15. Turn on the DC coupler and the oscilloscope, and start FUS pulses.

16. Monitor the voltage readout on the oscilloscope and adjust the position of the transducer in three axes using the stereotaxic manipulator until the voltage of corresponding FUS pulses reaches the maximum.

17. Repeat the measurements three times and record the maximum voltage V.

18. Increase the FUS pulse amplitude to 50% with 5% increments and repeat Step 17 in each setting.

19. Find the sensitivity M of the needle hydrophone at the frequency of the FUS transducer from the hydrophone calibration data provided by the manufacturer.

20. Calculate the peak pressure P of each measurement with the formula $P = V/M$.

21. Plot the calculated peak pressure as a function of the drive amplitude of FUS and fit the values with linear regression.

22. Save the calibration plot relating the drive amplitude and peak pressure of FUS for future reference. A reference plot showing the measured pressure and power density of the 1.5-MHz transducer as functions of the transducer amplitude can be found in Extended Data Fig. 2.

TROUBLESHOOTING

23. To investigate the spatial resolution of the FUS transducer, acquire a 2D (x-y or x-z) pressure map by moving the transducer in desirable dimensions. Specifically, first move the transducer from its starting position in the y direction within the range of ±5 mm with an interval of 0.2 mm and repeat Step 20 with a constant FUS amplitude (30%) at each step.

    CRITICAL The starting position ($x_0 = 0$, $y_0 = 0$, $z_0 = 0$) of the FUS transducer is determined in Step 16.

24. Next, move the transducer back to its starting position before moving it in the x direction within the range of ±5 mm with an interval of 0.2 mm. Repeat Step 23 for each x position.

25. Finally, to evaluate the pressure with respect to the distance between the tip of the needle hydrophone and the transducer (i.e., in the z direction), first move the transducer back to its starting position, then move the transducer axially to the needle hydrophone within the range of ±10 mm with an interval of 0.2 mm, and repeat Step 20 with a constant FUS amplitude (30%) at each step.

26. Move the transducer back to its starting position before moving it in the x direction within the range of ±5 mm with an interval of 0.2 mm. Repeat Step 25 for each x position.

27. Plot the 2D pressure map in the x-y plane (at $z_0 = 0$) based on the measurements in Steps 23-24. Plot the 2D pressure map in the x-z plane (at $y_0 = 0$) based on the measurements in Steps 25-26.

28. Save the spatial mapping plots of the FUS transducer for future reference. Representative pressure mapping results of a 1.5 MHz FUS transducer in the x-y

plane (at $z_0 = 0$) and in the x-z plane (at $y_0 = 0$) can be found in Extended Data Fig. 3a and 3b, respectively.

Spectral characterizations of ultrasound-mediated light emission in the phantom Timing 2 h

CRITICAL Fig. 5d shows a schematic illustration of the spectral characterization setup described in Steps 29-33.

29. Fill the transducer housing with ultrasound gel until the gel level surpasses the height of the housing. Place the phantom prepared from Step 7 on the ultrasound gel.

CRITICAL STEP Make sure there are no air bubbles in the ultrasound gel between the FUS transducer and the phantom.

30. Couple one end of the optical fiber to the spectrometer and the other end with a collimating lens.

31. Place a vertical post near the transducer and place a post clamp on it.

32. Mount the collimating lens to a horizontal post with a post clamp and connect the horizontal post to a vertical post. Make sure that the bottom of the collimating lens is close to the PDMS phantom .

CRITICAL STEP The joint between the horizontal post and the vertical post should be loose to facilitate the rotation of the horizontal post.

33. Place a “stop” post to confine the rotation angle of the horizontal post such that the center of the transducer and that of the collimating lens are vertically aligned when the two posts are in contact. A complete experimental setup can be found in Fig. 5e, where we define the current position of the lens-coupled fiber as Position 1 (Fig. 5f).

34. Open the OceanView software and set the software for time-series spectrum acquisition.

35. In the View mode, click the “Configure graph saving” button and select “Time Series (column data)” as the file format.

36. In the Acquisition Group Window, check the “Burst Mode” and set the integration time to 100 ms and the number of “Spectrum back to back” to 50~75, which corresponds to a total acquisition time of 5~7.5 s.

37. Connect the FUS system to the computer with a USB-to-USB-Type-B cable for FUS generation.

38. Turn on the FUS hardware and open the BBBop software. Load the FUS setting as follows: amplitude, 30%; pulse duration, 200 ms; and delay, 800 ms.

39. Move away the lens-coupled fiber from the center of the transducer to Position 2 (Fig. 5g).

40. Verify the charging light is aimed at the PDMS phantom. Adjust the position and the angle of the UV-LED lamp to ensure uniform light illumination.

41. Measure the power of the UV-LED lamp with an optical power meter and adjust the controller to set the incident power density on the PDMS phantom to 0.5 mW/mm^2.

42. Turn off the room light and start charging with the UV-LED lamp for 10 s.

    CRITICAL STEP It is important to move the fiber to Position 2 during charging to avoid saturation or damage to the spectrometer during charging.

43. After charging, immediately move the lens-coupled fiber over the PDMS phantom (Position 1) and start time-series spectrum acquisition.

44. Start FUS pulses. The time-series spectra will be saved automatically.

45. Compute the mechanoluminescence spectrum by subtracting the baseline spectrum, which corresponds to the spectrum taken immediately before the FUS pulse, from the peak spectrum, which corresponds to the spectrum taken during maximum emission under an FUS pulse. Normalized mechanoluminescence spectra of MLNTs of $Sr_2MgSi_2O_7$:Eu,Dy, ZnS:Cu,Al, ZnS:Mn, and $CaTiO_3$:Pr can be found in Extended Data Fig. 4.

TROUBLESHOOTING

PAUSE Researchers may pause here and continue the following steps later.

Spatial characterizations of ultrasound-mediated light emission in the phantom Timing 1 h

CRITICAL Fig. 5h shows a schematic illustration of the spatial characterizations setup described in Steps 46-49.

46. Place the phantom on the FUS transducer as described in Step 29.

47. Mount a camera above the phantom. Make sure the camera is horizontal with a spirit level (Fig. 5i).

48. Connect the camera to the computer using a USB-to-USB-B micro superspeed cable for image acquisition.

49. Open the ThorCam software and adjust the relative position between the phantom and the camera to make sure that a clear phantom image forms in the center of the camera's field of view.

50. Set the imaging acquisition parameters of the camera: exposure time, 50 ms; gain, 0; binning factor, 4.

51. Check if the camera blocks the charging light of the UV-LED lamp. Adjust the position and the angle of the UV-LED lamp if necessary.

52. Set up the FUS system as described in Steps 37-38.

53. Turn off the room light, and start the UV-LED lamp charging for 10 s.

54. After charging, immediately start time-series image acquisition and FUS pulses.

CRITICAL STEP When acquiring the images, make sure that no pixels are saturated on the camera. Additionally, to obtain the optimal imaging result, it is important to start FUS pulses immediately after charging as most of the stored energy will gradually be released via a thermal process.

55. Save the time-series images as a multipage tiff file.

56. Obtain the line profile of the emission spot using the ImageJ software.

57. Fit the emission line profile with a Gaussian function. The spatial resolution of FUS-mediated light emission is defined as the full-width-at-half-maximum (FWHM) of this fitted Gaussian function. An example of acquiring the emission line profile and Gaussian fitting can be found in Extended Data Fig. 5.

PAUSE POINT Researchers may pause here and continue the following steps whenever needed.

Rechargeability measurements of ultrasound-mediated light emission in the phantom Timing 1 h

58. Place the phantom on the FUS transducer as described in Step 29.

59. Set up the camera over the phantom as described in Steps 47-49.

60. Set up the FUS system as described in Steps 37-38.

61. Connect the analog output ports of the multifunction I/O device to the UV-LED lamp controller and FUS hardware (“Trigger-in” for both) via BNC-to-BNC cables.

CRITICAL STEP Port 0 should be connected to the UV-LED lamp, and Port 1 should be connected to the FUS system, consistent with the Matlab code.

62. Open the BBBop software, switch “all measurements” to “no measurement”, and set the FUS system to “trigger pulse”.

63. Run a test trial by setting the cycle number in the Matlab code to be 1 and run the code. A single time-series tiff file will be saved automatically. A representative tiff file can be found in Data availability.

CRITICAL STEP In the custom-written Matlab code, each cycle consists of 5-s charging and 7.5-s image acquisition (49.966-ms exposure time, 20-Hz frame rate, 150 frames in total) with a 2-s interval in between. FUS pulses start at 2 s after the start of image acquisition. The interval between consecutive cycles is 5.5 s.

TROUBLESHOOTING

64. Verify that emission can be clearly seen and that no pixels are saturated in the image.

65. Change the cycle number in the Matlab code to 50 and run the code. Representative rechargeability curves of MLNTs composed of $Sr_2MgSi_2O_7$:Eu,Dy, ZnS:Cu,Al, ZnS:Mn, and $CaTiO_3$:Pr over 20 cycles can be found in Extended Data Fig. 6.

66. (Optional) Since this procedure takes around 30 min, researchers may leave the room, leaving the rechargeability test operated automatically. Make sure that the room is kept in the dark during the entire experiment.

    PAUSE POINT Researchers may pause here and continue the following steps later.

Procedure 3 Characterizations of MLNTs in an artificial circulatory system

Construction of the artificial circulatory system Timing 30 min

CRITICAL STEP Fig. 6a shows a schematic illustration of the artificial circulatory system.

1. Fill the transducer housing with ultrasound gel and 3D-print a holder that can be tightly mounted on the transducer housing while leaving two openings on the opposite sides of the circular frame. A STL file of the holder can be found in Data availability.

2. Insert the tubing, which has an inner diameter of 1.59 mm, an outer diameter of 3.18 mm, and a total length of 35 cm, through the 3D-printed holder. Mount the holder on top of the transducer (Fig. 6b) and make sure there is no air between the transducer and the tubing.

3. Assemble the tubing to the peristaltic pump and set the flow rate of the pump to 11.3 ml/min.

4. Prepare 1.5 ml of an MLNT colloidal solution at a concentration of 40 mg/ml in a 2 ml glass vial. Add a stir bar in the vial.

5. Place the glass vial on a magnetic stirrer and secure it with a flask clamp.

6. Insert the two ends of the tubing into the glass vial and make sure the openings of the tubing are fully immersed in the colloidal solution (Fig. 6c).

Temporal dynamics of ultrasound-mediated light emission in the artificial circulatory system Timing 2 h

7. Connect the UV-LED with a DC power supply.

8. Mount the UV-LED on the optical table and adjust the controller to set the power density to 3.8 mW/mm^2.

9. Place the tubing on top of the LED chip. Secure the tubing in place with tapes (Fig. 6d).

10. Mount a camera above the 3D-printed holder with tubing inside and make sure the camera is horizontal with a spirit level (Fig. 6e).

11. Connect the camera to the computer via a USB-to-USB-B micro superspeed cable for image acquisition.

12. Open the ThorCam software and adjust the relative position between the tubing and the camera to make sure that a clear tubing image forms in the center of the camera's field of view.

13. Set the image acquisition parameters of the camera: exposure time, 5 ms; gain, 0; binning factor, 4.

14. Connect the FUS system to the computer via a USB-to-USB-Type-B cable.

15. Turn on the FUS hardware and open the BBBop software.

16. Load the FUS settings and set the FUS pulse width to 10 ms.

CRITICAL STEP To investigate the temporal dynamics of the ultrasound-mediated light emission in the artificial circulatory system, change the FUS pulse width from 10 to 50 ms. The amplitude (30%) and the repetition rate (1 Hz) remain constant. In our experiments, we find that varying the FUS pulse width from 10, 20, to 50 ms is sufficient to study the temporal dynamics of ultrasound-mediated light emission in the artificial circulatory system.

17. Turn on the magnetic stirrer and the peristaltic pump. Make sure the flow of MLNT colloidal solution is continuous inside the tubing.

18. Seal the light leakage from the UV-LED and the illuminated segment of the tubing with black aluminum foil (Fig. 6f).

19. Turn off the room light, turn on the UV-LED, and make sure the camera does not capture any stray light.

20. Start image acquisition and FUS pulses.

CRITICAL STEP The tubing filled with the MLNT colloidal solution under FUS stimuli should exhibit bright emission at the focus of ultrasound as shown in Fig. 6g-j.

21. After the first session of FUS, adjust the FUS pulse width accordingly.

22. For each experimental condition, repeat the measurements several times and average the onset and offset times of FUS-mediated light emission, which correspond to the time delay of light emission after the FUS pulse is applied and removed, respectively. Expected temporal kinetics of FUS-mediated light emission from mechanoluminescent fluids composed of $Sr_2MgSi_2O_7$:Eu,Dy, ZnS:Cu,Al, ZnS:Mn, and $CaTiO_3$:Pr can be found in Extended Data Fig. 7.

CRITICAL STEP The onset time is defined as the time between the start of FUS pulse (t_1) and the time (t_2) when the light intensity (I) has increased to three times the standard deviation of I before t_1. The offset time is defined as the time between the end of the FUS pulse (t_3) and the time (t_4) when I has dropped below three times the standard deviation of I at infinite time.

23. After the test, turn off the magnetic stirrer, the peristaltic pump, and the UV-LED, and turn on the room light.

TROUBLESHOOTING

Absolute emission intensity measurement of the ultrasound-mediated light source in the artificial circulatory system Timing 1 h

24. Determine the radius of the emission spot, r, in the artificial circulatory system by repeating Procedure 2 Steps 56-57.

25. Replace the camera with a photodiode which is connected to the photodiode amplifier.

26. To calculate the tubing's transmittance T, follow these steps: Set up a stable light source, such as a LED, that matches the wavelength of the tested MLNTs, and position the photodiode in front of this light source to measure the light intensity I_1. Next, slice the tubing lengthwise and flatten it so it can cover the photodiode's sensing area. Measure the light intensity of the light source, I_2, with the tubing covering the photodiode. Finally, calculate the tubing's transmittance T at this specific wavelength using the formula $T = \frac{I_2}{I_1}$.

27. Connect the output from the photodiode amplifier to an analog input port (AI 0) of the multifunction I/O device with a BNC-to-BNC cable.

28. Load the FUS settings and set the pulse width to 200 ms, amplitude to 30%, and the repetition rate to 1 Hz.

29. Open the LabVIEW software and open the file "PD.vi". Set the optical power acquisition parameter as follows: sampling frequency, 1000; binning factor, 10.

30. Repeat Steps 17-18 to set up the artificial circulatory system.

31. Turn off the room light, turn on the UV-LED, and make sure the readings from the photodiode remain unchanged after the UV-LED is turned on. This step is to ensure that the photodiode does not capture any light leakage from the UV-LED.

32. Start the optical power measurement of light emission from the artificial circulatory system and start FUS pulses.

33. Save the power measurements in excel files.

34. Calculate the optical power density (I_0) according to $I_0 = \frac{d^2}{TAr^2} P_m$, where d is the distance between the emission spot and the sensor of the photodiode, T is the transmittance of the tubing at the peak wavelength of the tested MLNTs (Table 1), A is the sensing area of the photodiode, r is the radius of the emission spot in the artificial circulatory system, P_m is the measured power of light emission by the photodiode. For reference, the calculated I_0 of the mechanoluminescent fluid composed of $Sr_2MgSi_2O_7$:Eu,Dy at a concentration of 25 mg/ml is 0.7 mW/cm^2 with a variation of 6.8% between repeated measurements.

Pressure-to-luminance transfer functions of ultrasound-mediated light emission in the artificial circulatory system Timing 2 h

35. Keep the magnetic stirrer, the peristaltic pump, and the UV-LED on. Keep the room light off.

36. Set the FUS pulse width as 200 ms and the repetition rate as 1 Hz.

37. Set the drive amplitude of the FUS as 5%, which corresponds to a certain peak pressure obtained from the calibration plot from Procedure 2, Step 22.

38. Start image acquisition and apply FUS pulses.

39. Gradually increase the FUS amplitude and repeat Step 37 for each drive amplitude.

40. Determine the threshold pressure for the MLNTs to produce light emission by plotting the measured emission intensity from each captured image vs its corresponding FUS pressure. Expected dependence of the emission intensity from mechanoluminescent fluids composed of $Sr_2MgSi_2O_7$:Eu,Dy, ZnS:Cu,Al, ZnS:Mn, and $CaTiO_3$:Pr on FUS pressure can be found in Extended Data Fig. 8.

Procedure 4 Using deLight for *in vivo* sono-optogenetic neuromodulation

CRITICAL MLNTs, which exhibit strong emission under FUS and consistent emission under repeated charging and discharging cycles, must be prepared before any *in vivo* applications of deLight. Researchers can choose either tail vein injection (option 1) or retro-orbital injection (option 2) for systemic delivery of the MLNT solution (Fig. 7a).

Using deLight for *in vivo* optogenetic neuromodulation Timing 1-5 h

1. Prepare and sterilize the procedure area and surgical tools (Fig. 7b).

CAUTION All procedures involving live animals must be approved by the institution’s Animal Care and Use Committee.

2. (Optional) Mount a video-recording device for monitoring mouse limb movements. Add a lens tube to the UV-LED lamp for better spatial confinement of the recharging area (Fig. 7c).

CRITICAL STEP This step is only required for the behavioral assay.

3. Anesthetize a mouse by intraperitoneally injecting the anesthetic mixture. The anesthesia level of the mouse should be checked by assessing the paw withdrawal reflex in response to a toe pinch.

CRITICAL STEP Follow option a if a behavioral assay will be performed. Follow option b if brain c-fos expression levels will be evaluated.

a. Behavioural assay

i. Administer the anesthetic drug at a dose of 1 μl/g. The animal should show the paw withdrawal reflex in response to a toe pinch.

b. C-fos expression evaluation

i. Administer the anesthetic drug at a dose of 5 μl/g and a maximum dosage of 150 μl regardless of the animal's weight. The animal should show no paw withdrawal reflex in response to a toe pinch.

4. Remove the fur of the mouse with hair removal lotion.

CRITICAL STEP If a behavioral assay is performed, remove the fur on the head, entire back, hindlimbs, and hindpaws of the mouse. If only post-mortem immunostaining of brain sections will be performed, remove the fur on the head and the lower back of the mouse.

5. Apply a small amount of eye lubricant to each eye to prevent drying during this procedure.

6. (Optional) Mark the joints of both hindlimbs with four different colors (Fig. 7d).

CRITICAL STEP This is only required for the behavioral assay. Try to mark those regions as symmetric as possible.

7. Place the animal on a heating pad set to 37 °C to prevent hypothermia.

CRITICAL STEP If a behavioral assay is performed, skip Step 8 and proceed to Step 9. If researchers intend to evaluate c-fos expression, proceed to Step 8.

8. (Optional) Wait for 2 h before proceeding to the next step. During the wait, apply additional eye lubricant as needed.

CRITICAL STEP This step is crucial for reducing and even eliminating the baseline c-fos expression in the targeted brain region. Based on our experience, 2 h is sufficient for producing a clean c-fos background in the absence of neural stimulation. Researchers can adjust the time as needed.

9. Mount the mouse head to the head holder by placing the mouse's front teeth into the inner hole of the head holder and tightening the placement with the screw.

10. Place the ear bars into the mouse's ear canal and tighten the ear bars with screws in place. CRITICAL STEP This step is essential for setting the right coordinates for later procedures.

11. Adjust the position and the angle of the UV-LED lamp to make sure part of the mouse's back is illuminated according to the following instructions.

CRITICAL STEP If a behavioral assay is performed, adjust the relative position of the UV-LED lamp and the video recording device to make sure the lower body of the animal (i.e., the area that is captured by the video recording device) is not illuminated. The illumination area in the behavioral assay should be the upper back of the animal, thus justifying the removal of fur on the entire back in Step 4. If only post-mortem immunostaining of brain sections will be performed, the shaved lower back of the animal should be illuminated.

12. Measure the power of the UV-LED lamp with an optical power meter and adjust the controller to set its output power to 1 mW/mm^2.

13. Connect the FUS system to the computer with a USB-to-USB-Type-B cable for FUS stimulation.

14. Turn on the FUS hardware, open the BBBop software, and connect the stereotaxic manipulator with the mounted FUS transducer to control the movement of the transducer.

15. Lift the scalp with forceps and make an incision with scissors.

16. Clean the exposed skull with 1x PBS and mark the bregma with a sharpie (Fig. 7e). The incision of the scalp and exposure of the skull are only intended for generating deLight at precise stereotaxic coordinates with respect to the bregma in the skull. FUS can penetrate through the intact mouse scalp and skull with minimal attenuation, thus not requiring their removal for producing light emission in the brain.

17. Use a spirit level to make sure the transducer is horizontal (Fig. 7f).

18. Place a small piece of $Sr_2MgSi_2O_7$:Eu,Dy-doped PDMS phantom (refer to Procedure 2) on the FUS transducer housing, which is filled with ultrasound gel, and charge it with a UV flashlight.

19. Turn off the room light and turn on FUS. Mark the bright point (Fig. 7g) in the phantom with a sharpie as the focus of the FUS transducer (Fig. 7h&i).

    TROUBLESHOOTING

20. Place an “L” shaped aligner consisting of one post and one needle to align the lateral position of focus of the transducer with one arm (i.e., attached needle) of the aligner (Fig. 7j).

21. Rotate the transducer together with the aligner from an upward-facing position to a downward-facing one.

22. Align the marked bregma (from Step 16) of the mouse with the needle tip (Fig. 7k) by moving the transducer laterally until the needle tip aligns with the mouse’s bregma. This approach ensures that the FUS transducer’s focus shares the AP and ML coordinates with the bregma.

    CRITICAL STEP Make sure after the rotation, the transducer stays horizontal with a spirit level. This step aligns the focus of the transducer with the bregma of the mouse brain, and in this way the alignment achieves its highest possible accuracy.

23. Remove the aligner and the phantom.

24. Apply extra ultrasound gel to the transducer and the animal’s exposed skull (Fig. 7l).

25. Move the transducer with the stereotaxic manipulator to the targeted coordinates with respect to the bregma in both *x* and *y* directions.

CRITICAL STEP The reference coordinates can be found at Mouse Brain Atlas (http://labs.gaidi.ca/mouse-brain-atlas/) and Reference Atlas (https://mouse.brain-map.org/static/atlas). Researchers should choose the stereotaxic coordinates according to their specific studies. The mouse skull exhibits a negligible effect on shifting the focus of ultrasound (within the frequency range of 1.5 - 6 MHz),[41] thus enabling the use of deLight without significant off-target effect in the mouse brain without adjusting stimulation coordinates.

26. Slowly lower the transducer by adjusting its height until the "ring" of the transducer housing is (*f-t-DV*) mm away from the exposed skull, where *f* corresponds to the the focal length of the FUS transducer, *t* the thickness of the housing, and *DV* the dorsal-ventral coordinate of the target brain region (Fig. 7m). A representative side view of the relative position of the transducer and the mouse head is shown in Fig. 7n.

CRITICAL STEP When lowering the transducer, researchers should use a caliper to measure the distance between the edge of the transducer housing (i.e., the "ring") and the surface of the skull to match the desired value of (*f-t-DV*) mm.

CAUTION Avoid causing damage to the animal when lowering the transducer.

27. (Optional) Lift the transducer by 10 cm via the stereotaxic manipulator of the FUS system. CRITICAL STEP This is only required if the retro-orbital injection is performed in 30.

28. Prepare 200 μl of the MLNT colloidal solution in 1x PBS (30 mg/ml) and load the solution into a 29 gauge insulin syringe.

29. (Optional) Adjust the position of the video recording device to make sure the lower body of the mouse with the markers can be clearly seen before starting video recording. CRITICAL STEP This is only required for the behavioral assay.

30. Charge the MLNT solution with a UV flashlight and perform systemic administration. Researchers can either perform tail vein injection (Fig. 7o) or retro-orbital injection (Fig. 7p).

31. After the injection, immediately turn on the UV-LED lamp for recharging on the animal's skin.

32. (Optional) Lower the transducer by 10 cm to reach the preset brain coordinates for the targeted region with the stereotaxic manipulator (Fig. 7q).

CRITICAL STEP This is only required if retro-orbital injection is performed in 30.

33. Start the first FUS pulse train for 5 min (amplitude 25%, pulse duration 200 ms, and delay 800 ms).

CRITICAL STEP Due to the circulation half-life of systemically administered MLNTs, it is recommended to start the first FUS pulse train immediately after the administration of the MLNT fluids.

34. Start a timer of 30 s after the first session is finished and start the second session for 5 min (amplitude 25%, pulse duration 200 ms, and delay 800 ms) at the end of the 30-s interval. CRITICAL STEP The UV-LED lamp should be turned off during the 30-s interval and turned back on when the second FUS session starts. If the researchers plan to change the duration of the FUS stimulation, ensure that the total duration combining Step 32, 33, and 34 is within 30 min after MLNT administration.

35. (Optional) Stop video recording.

    CRITICAL STEP This is only required for the behavioral assay.

36. Remove the mouse head from the head holder and close the wound with Vetbond (Fig. 7r). CRITICAL STEP If a behavioral assay is performed, proceed to Step 37. If researchers intend to evaluate c-fos expression, proceed to Step 38.

37. (Optional) Inject a dose of an anti-sedative drug and monitor the animal's health condition according to the approved animal protocol. Analyze the recorded limb motion with a customized Matlab code.

    CRITICAL STEP This is the last step if the deLight behavioral assay is performed. If researchers intend to evaluate the c-fos expression level, proceed to Step 38.

38. (Optional) Wait for 90 min for c-fos expression.

    CRITICAL STEP During the wait, prepare the procedure area and tools for transcardial perfusion. Apply eye lubricant as needed.

Perfusion, tissue collection, and fixation Timing 2 d

CRITICAL The following Steps 39-82 are for c-fos evaluation only.

39. Place the animal on the dissection stage inside a fume hood.

    TROUBLESHOOTING

40. Perform a midline laparotomy to expose the heart.

    CRITICAL STEP Avoid causing damage to inner organs, especially the heart.

41. Insert a 27 gauge needle into the left ventricle and make a small incision on the right atrium. Perfuse the animal with 15 ml of 1x PBS through the inserted needle at a rate of 5 ml/min.

42. Following 1x PBS perfusion, perfuse the animal with 25 ml of 4% (wt/vol) PFA.

43. Collect the brain from the skull and post-fix it in 4% PFA at 4°C for 24 h.

44. Remove the brain from PFA and rinse it with 1x PBS. Place the brain in the brain slicer (Fig. 8a). Use razor blades to collect coronal sections with ca. 3 mm thickness around the region of interest (Fig. 8b).

    CRITICAL STEP Make sure that the ventral side of the brain faces upwards. This orientation ensures that the cutting plane is roughly parallel to the standard

brain atlas. Before the cut, reference the brain atlas and determine the locations of the cut. Increase the brain section thickness to avoid missing the region of interest if necessary.

45. After collecting the desired brain section, cut a small piece of brain tissue from the bottom of the non–FUS-stimulated cerebral hemisphere.

CRITICAL STEP This step marks the side of the mouse brain not illuminated with deLight to facilitate immunostaining and imaging of c-fos later.

46. Put the brain section of interest in 10 ml of 0.1 M PB solution containing 30% sucrose at 4 °C until the tissue block sinks to the bottom.

CRITICAL STEP The brain tissue will float in the sucrose solution when first immersed (Fig. 8c), before sinking to the bottom overnight (Fig. 8d). If the tissue section is thicker than 3 mm, a longer time is needed before the tissue block sinks to the bottom. Researchers may replace the sucrose solution with freshly made solutions to expedite the diffusion process.

Frozen embedding and sectioning of brain tissue Timing 2 h

47. Prepare materials and tools needed for tissue sectioning. First, take the brain tissue out from the sucrose solution, and wipe off the remaining solution from the surface with Kimwipes.

48. Transfer the brain tissue into a plastic mold prefilled with a thin layer of O.C.T. compound with blunt forceps. Add extra O.C.T. compound to fill the mold and put the plastic mold on ice for 30 min.

CRITICAL STEP To avoid drying of the O.C.T. compound, it is preferable to place the mold inside a styrofoam container. Also avoid the formation of air bubbles. If there are any air bubbles, remove them with blunt forceps. Be careful not to damage the tissue.

49. During the 30 min wait, place a 10 cm petri dish on top of a foam box (which provides thermal insulation) and prepare a slurry composed of dry ice and methanol in the petri dish.

50. Repeat Step 46 to transfer the brain tissue to a second plastic mold.

51. Use long forceps to grasp the mold and place it into the dry ice-methanol slurry. After all the O.C.T. compound has turned white, transfer the mold to dry ice.

CRITICAL STEP Make sure that the mold floats on the surface of the dry ice-methanol slurry, so that methanol is not in contact with O.C.T. compound or tissue. O.C.T. compound should turn white when it freezes within 1-2 min (Fig. 8e).

PAUSE The tissue block can be stored at −80 °C for up to 6 months.

52. Transfer the tissue block to the precooled cryostat (Fig. 8f).

CRITICAL STEP During the transfer, always keep the tissue block on dry ice. Do not thaw the mold at room temperature.

53. Remove the solid block from the plastic mold and glue the tissue block to the sample holder with O.C.T. compound. Wait till the sample equilibrates to the chamber temperature. CRITICAL STEP If the tissue block is freshly frozen-embedded, wait for 30 min. If the tissue was stored in the −80 °C freezer, wait for at least 1 h.

54. Mount the sample and the blade to the cryostat. Adjust the angle of the tissue block and the blade as needed.

CAUTION Pay extra attention to the sharp blades to avoid injuries.

55. Cut the tissue block into sections with a thickness of 40 μm and collect the sections of interest (Fig. 8g) into a 48-well plate filled with pre-cooled 1x PBS if the sections will be stained within two days.

PAUSE POINT Replace the 1x PBS with cryoprotectant for long-term storage. Sections can be stored at −20 °C for up to 6 months.

Immunostaining, mounting, and imaging Timing 2-3 d

56. Prepare the tools and materials needed for immunostaining.

57. Mark brain sections from the original 48-well plate and transfer the ones selected for immunostaining with a paintbrush into a new well plate pre-filled with 1x PBS.

CRITICAL STEP Pay extra attention to the transfer process to avoid damage to the brain sections.

58. Put the shaker inside a 4 °C fridge. Rinse the brain sections in 1x PBS for 10 min on the shaker at a speed of 450 rpm. Repeat 3 times.

CRITICAL STEP After each rinse, transfer the brain sections to a new well filled with fresh solution, or discard the old solution with a pipette. This step applies to Steps 58-63.

59. Block each brain section in 200 μl of the blocking solution for 1 h at room temperature on a shaker at a speed of 150 rpm.

60. Incubate each brain section in 200 μl of the primary antibody solution at 4 °C overnight on a shaker at a speed of 150 rpm.

61. Rinse each brain section in 500 μl of the washing solution three times for 10 min at 4 °C on a shaker at a speed of 450 rpm.

62. Incubate each brain section in 200 μl of the secondary antibody solution at room temperature for 1.5 h on a shaker at a speed of 150 rpm.

CRITICAL STEP The procedures involving secondary antibody solutions require light blockage. Perform all steps involving secondary antibodies with the samples covered in aluminum foil.

63. Rinse the brain section by repeating Step 58.

64. After the final rinse, transfer the as-stained brain sections to glass slides.

CRITICAL STEP Avoid wrinkles and folds during the transfer. Adding a droplet of 1x PBS will facilitate the transfer process.

65. Remove excess liquid and add a few drops of mounting medium.

66. Place a clean coverslip on the top of the brain section. Avoid air bubbles.

67. Remove excess mounting medium and seal the edges of the cover slip with nail polish (Fig. 8h).

68. Place the glass slide horizontally in a microscope slide storage folder, allowing the nail polish to dry in the dark for at least 2 h before imaging.

PAUSE POINT The prepared brain sections can be stored at room temperature up to 1 month. Based on our experience, a delay in subsequent imaging may increase the autofluorescence signal. It is thus recommended that confocal imaging be performed within one week after the preparation.

69. Turn on the confocal imaging system and place the tissue-mounted glass slide on the microscope stage.

70. Locate the cerebral hemisphere stimulated with deLight by referencing the cut made in Step 45.

71. Reference the brain atlas and find the brain region of interest.

72. Choose appropriate laser settings based on the excitation/emission wavelengths of the secondary antibody used for c-fos staining and those of the reporter for ChR2.

73. Image the brain region of interest with a *z*-stack.

TROUBLESHOOTING

CRITICAL STEP Avoid intensity saturation in the confocal images by adjusting imaging settings. The same imaging settings should be used in all control experiments.

74. Use appropriate software (e.g., ImageJ) to open the confocal images and quantify the number of cells with positive c-fos signals in each region of interest.

TROUBLESHOOTING

(Optional) Evaluating the volume of brain tissue optogenetically-activated by deLight based on immunostaining of c-fos Timing 1 d

75. Obtain a tile scan of the coronal brain section immunostained for c-fos.

76. Center on the region showing high c-fos signals.

77. Use image processing software (e.g., ImageJ) to segment the c-fos features in the original image.

78. Convert the image from Step 77 into a binary format, where '1' represents a pixel with a positive c-fos signal and '0' signifies a pixel without c-fos.

79. Project the binary c-fos image along its long axis, which corresponds to the dorsoventral (DV) axis of the brain section, to obtain a c-fos intensity profile.

80. Fit the intensity profile with a Gaussian function to determine the stimulated region's lateral radius (r), taken as the half-width at half-maximum of the fitted curve.

81. Determine the depth of the stimulated region (d) as the distance between the start and end depths of positive c-fos expression.

82. Calculate the volume of the stimulated brain region (V_{c-fos}) by applying the ellipsoid volume equation: $V_{c-fos} = \frac{2}{3}\pi r^2 d$.

Troubleshooting

Troubleshooting advice can be found in Table 3.

Timing

Procedure 1

Step 1-17, synthesis of bulk mechanoluminescent materials via solid-state reactions: 2 d

Step 18-21, synthesis of MLNTs via a biomineral-inspired suppressed dissolution approach: 3 d

Step 22-48, surface modification of biocompatible MLNTs: 2 d

Procedure 2

Step 1-7, preparation of the tissue-mimicking phantom uniformly doped with MLNTs: 1 h

Step 8-28, calibration of FUS transducers with a needle hydrophone: 1 d

Step 29-45, spectral characterizations of ultrasound-mediated light emission in the phantom: 2 h

Step 46-57, spatial characterizations of ultrasound-mediated light emission in the phantom: 1 h

Step 58-66, rechargeability measurements of ultrasound-mediated light emission in the phantom: 1 h

Procedure 3

Step 1-6, construction of the artificial circulatory system: 30 min

Step 7-23, temporal dynamics of ultrasound-mediated light emission in the artificial circulatory system: 2 h

Step 24-34, absolute emission intensity measurement of the ultrasound-mediated light source in the artificial circulatory system: 1 h

Step 35-40, pressure-to-luminance transfer functions of ultrasound-mediated light emission in the artificial circulatory system: 2 h

Procedure 4

Step 1-38, using deLight for in vivo optogenetic neuromodulation: 1-5 h

Step 39-46, perfusion, tissue collection, and fixation: 2 d

Step 47-55, frozen embedding and sectioning of brain tissue: 2 h

Step 56-74, immunostaining, mounting, and imaging: 2-3 d

Step 75-82, evaluating the volume of brain tissue optogenetically-activated by deLight based on immunostaining of c-fos: 1 d

Anticipated results

This protocol provides a detailed description of the implementation of a non-invasive deep-tissue light delivery method, termed “deLight”. After the completion of this protocol, researchers will be able to synthesize the MLNTs with emissions spanning the entire visible spectrum under FUS, characterize the properties of MLNTs and deLight in tissue-mimicking phantoms and artificial circulatory systems, and apply deLight for any applications that need light in the deep tissue in live animals. Specifically, successfully produced MLNTs should have bright emissions and good colloidal stability when dispersed in an aqueous solution. Before applying deLight *in vivo*, researchers can use this protocol to characterize the emission spectra, spatial resolution, and temporal dynamics of synthesized MLNTs in tissue-mimicking phantoms and in an artificial circulatory system. Furthermore, *in vivo* implementation of deLight takes advantage of the endogenous circulatory system that allows these MLNTs to be recharged in the superficial vessels near the skin and discharged to produce local light emission at the ultrasound focus. As a representative example, this protocol describes a procedure of applying deLight for *in vivo* sono-optogenetic neuromodulation in live mice, followed by a behavioral assay (Fig. 7a) and an immunohistochemical assay (Fig. 7b) to validate efficacious light emission. Besides the demonstrated *in vivo* optogenetic application of deLight described in Procedure 4, we envision that this unique approach for systemic light delivery can facilitate minimally-invasive optogenetic neuromodulation in deeper brain regions in larger animals and enable any biological applications that require light in the deep body.

Extended Data

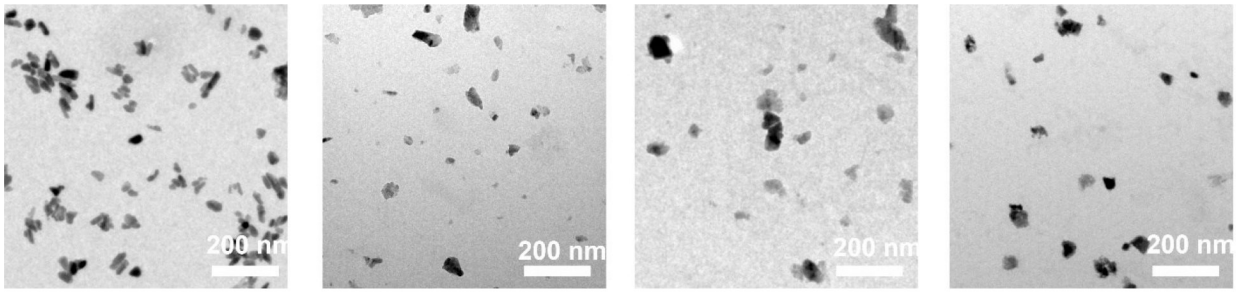

Extended Data Fig. 1.
Representative TEM images of colloidal MLNTs of $Sr_2MgSi_2O_7$:Eu,Dy, ZnS:Cu,Al, ZnS:Mn, and $CaTiO_3$:Pr. Reproduced with permission from Ref. 22.

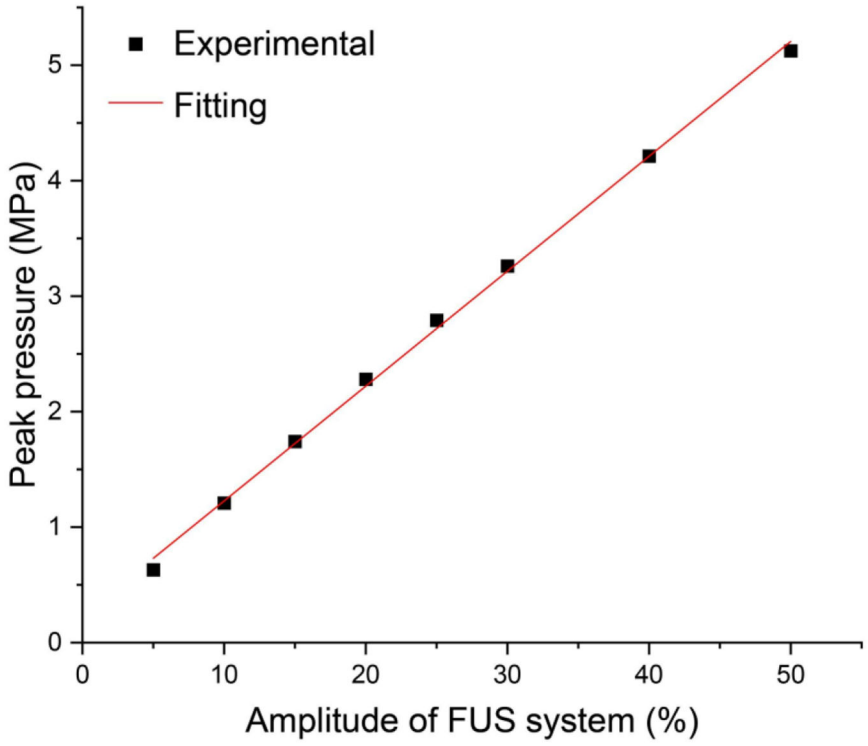

Extended Data Fig. 2.
Peak pressure measured by the hydrophone (black) plotted against the percent amplitude of the FUS system. Linear fitting (black) yields an empirical formula: $P = 0.1A + 0.2$, where P is the pressure in MPa and A is the amplitude in %. Reproduced with permission from Ref. 20.

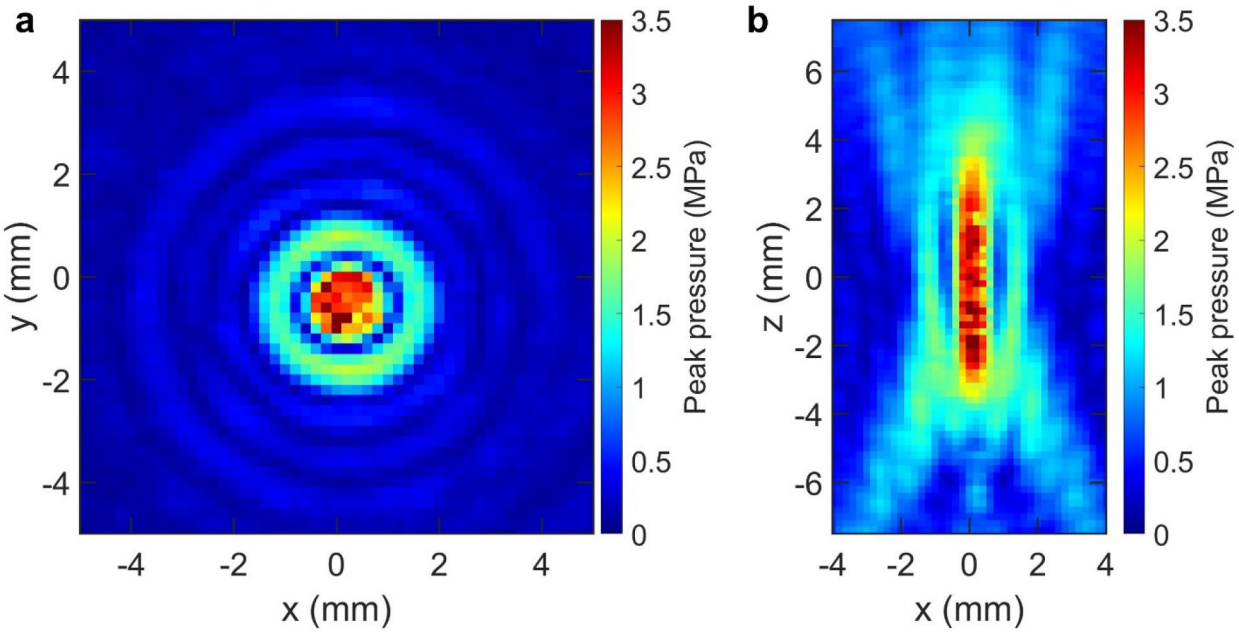

Extended Data Fig. 3.

Pressure mapping of the 1.5 MHz FUS transducer in the **a**, *x*-*y* plane (at $z_0 = 0$) and in the **b**, *x*-*z* plane (at $y_0 = 0$).

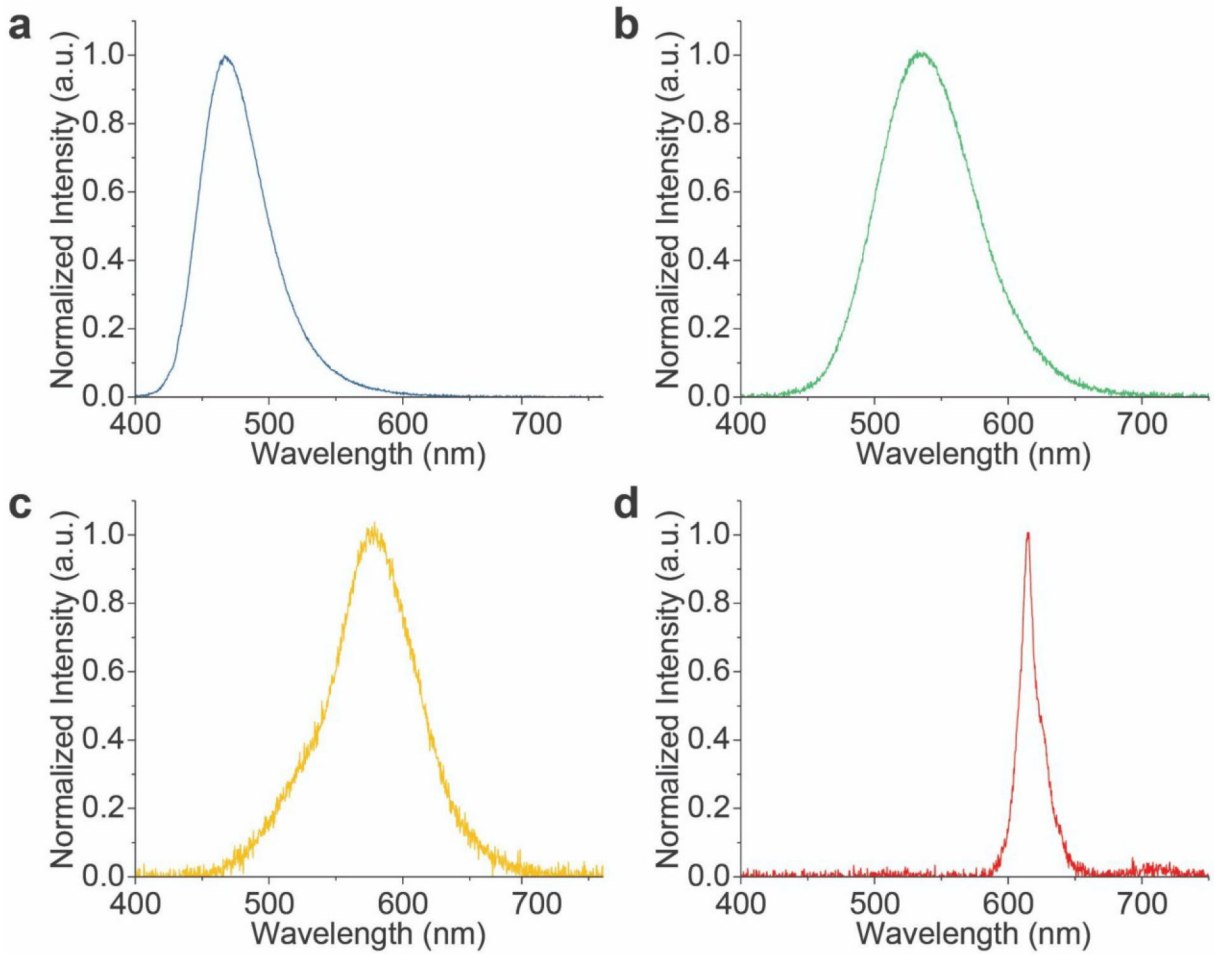

Extended Data Fig. 4.

Normalized mechanoluminescence spectra of MLNTs composed of $Sr_2MgSi_2O_7$:Eu,Dy (**a**), ZnS:Cu,Al (**b**), ZnS:Mn (**c**), and $CaTiO_3$:Pr (**d**). Adapted with permission from Ref. 22.

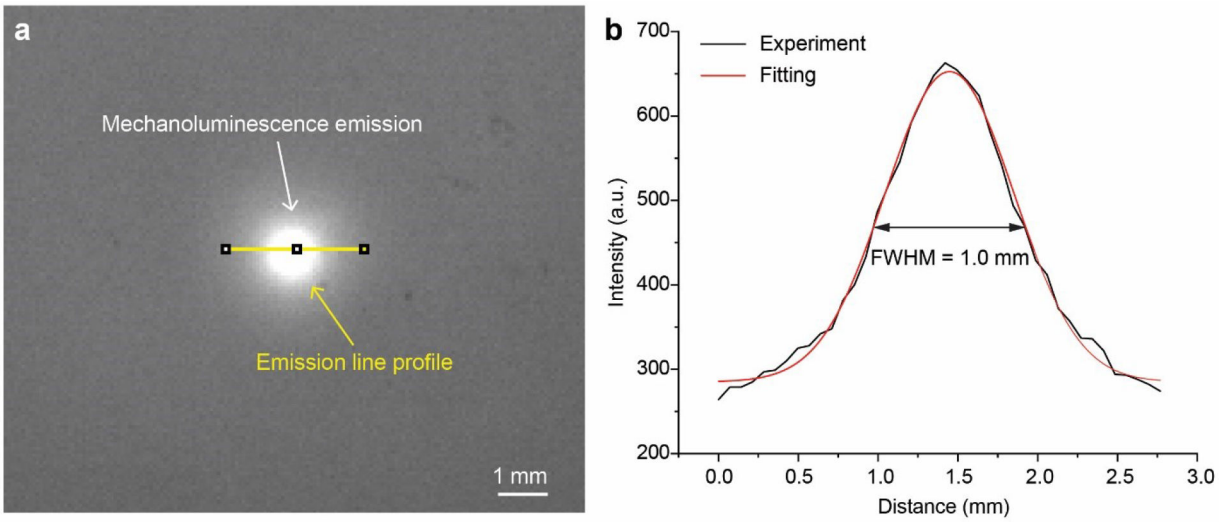

Extended Data Fig. 5.

An example mechanoluminescence image (**a**) and its corresponding emission line profile fitted to a Gaussian function (**b**) to obtain the FWHM.

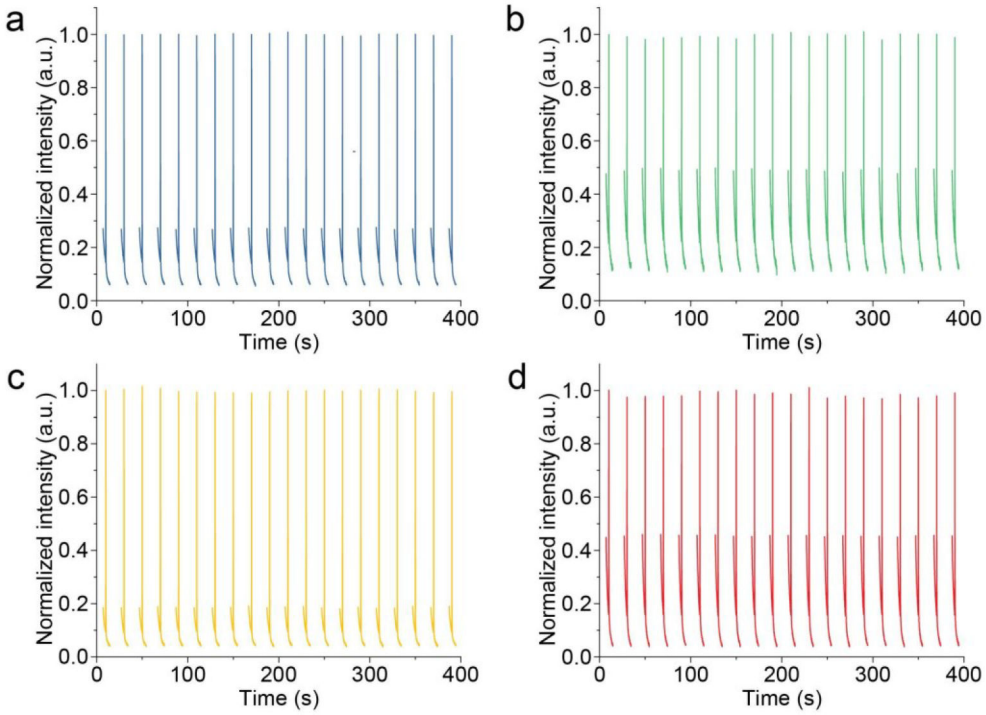

Extended Data Fig. 6.

Representative rechargeability curves of MLNTs composed of $Sr_2MgSi_2O_7$:Eu,Dy (**a**), ZnS:Cu,Al (**b**), ZnS:Mn (**c**), and $CaTiO_3$:Pr (**d**). Reproduced with permission from Ref. 22.

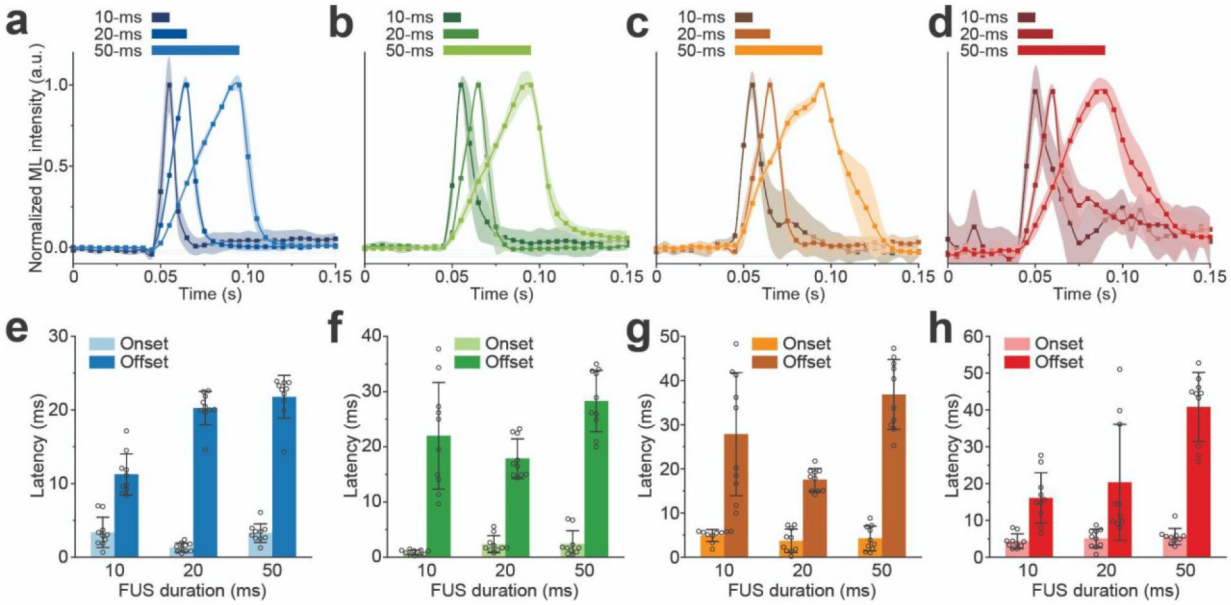

Extended Data Fig. 7.

Temporal kinetics of FUS-induced light emission from colloidal solutions of MLNTs. (**a–d**) Temporal kinetics of MLNT solutions composed of (**a**) $Sr_2MgSi_2O_7$:Eu,Dy, (**b**) ZnS:Cu,Al, (**c**) ZnS:Mn, and (**d**) $CaTiO_3$:Pr upon 10, 20, and 50 ms FUS pulses in the artificial circulatory system with an imaging frame rate of 200 Hz. (**e–h**) Onset and offset times of mechanoluminescence emission measured from (**a-d**). All data are presented as mean ± SD of 10 independent measurements. ML: mechanoluminescence. Reproduced with permission from Ref. 22.

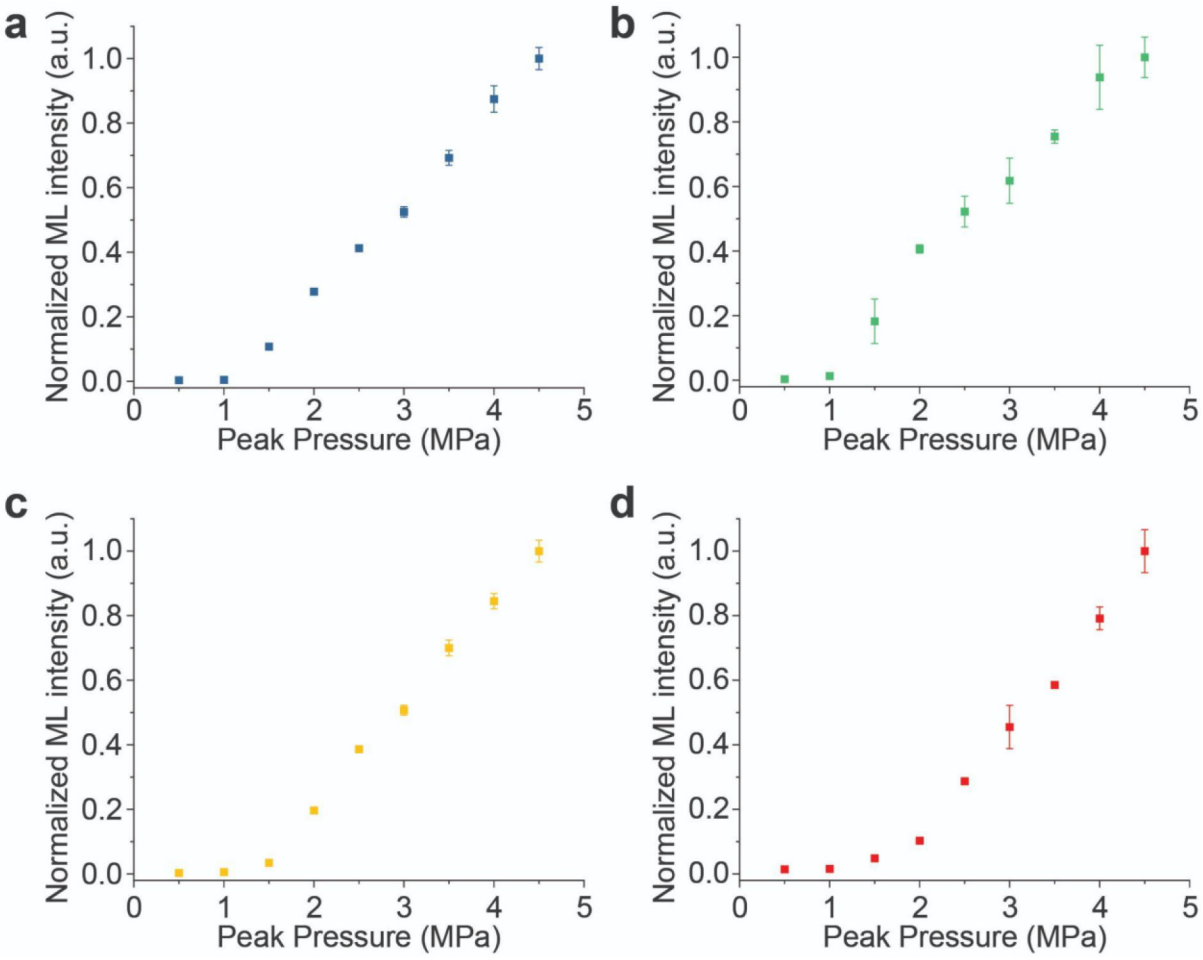

Extended Data Fig. 8.

Emission intensity from mechanoluminescent fluids composed of $Sr_2MgSi_2O_7$:Eu,Dy (**a**), ZnS:Cu,Al (**b**), ZnS:Mn (**c**), and $CaTiO_3$:Pr (**d**) under varying FUS pressure. Reproduced with permission from Ref. 22.

Acknowledgement

G.H. acknowledges two awards by NIH (5R00AG056636-04 and 1R34NS127103-01), an NSF CAREER award (2045120), an NSF EAGER award (2217582), a Rita Allen Foundation Scholars Award, a Beckman Technology Development Grant, a grant from the focused ultrasound (FUS) Foundation, a gift from the Spinal Muscular Atrophy (SMA) Foundation, a gift from the Pinetops Foundation, two seed grants from the Wu Tsai Neurosciences Institute, and a seed grant from the Bio-X Initiative of Stanford University. X.W. acknowledges the support by a Stanford Graduate Fellowship. N.J.R. acknowledges support from the NSF Graduate Research Fellowships Program (GRFP) and a Stanford Bio-X fellowship. Some schematics were created with BioRender.com.

Data availability

The source data for Extended Data Fig. 3-8 can be downloaded through the following link: https://doi.org/10.6084/m9.figshare.23690961. The STL file of the holder can be found in the following link: https://doi.org/10.6084/m9.figshare.23691309. A representative tiff file of the time series mechanoluminescence emission can be found in the following link: https://doi.org/10.6084/m9.figshare.23691312. Further data are available from the corresponding

author upon request. Characterized and quality-controlled MLNTs are available to other research labs upon request.

Code availability

The custom LabVIEW and MATLAB code used in this protocol is available at https://github.com/ShanJiang1233/deLight and is archived to Zenodo at https://doi.org/10.5281/zenodo.8162191.

KEY PAPERS

-At the start of the manuscript, please highlight up to 5 key references from your lab (including DOIs) that demonstrate the development/use of the protocol. This will be used in the related links section.

- We can also highlight 1 or more of these particular references in the ‘associated links’ box on the online article page if they are published in Springer Nature journals.

-You can categorize references as suitable to be listed as either ‘Key reference(s) using this protocol’ or containing ‘Key data used in this protocol (Optional heading)

Related links

Key references using this protocol:

References

1. Hong G. Seeing the sound. Science 369, 638 (2020): DOI: 10.1126/science.abd3636 [PubMed: 32764064]
2. Wu X. et al. Sono-optogenetics facilitated by a circulation-delivered rechargeable light source for minimally invasive optogenetics. Proc. Natl. Acad. Sci. U. S. A 116, 26332–26342 (2019): 10.1073/pnas.1914387116 [PubMed: 31811026]
3. Wang W. et al. Ultrasound-Triggered In Situ Photon Emission for Noninvasive Optogenetics. J. Am. Chem. Soc 145, 1097–1107 (2023): 10.1021/jacs.2c1Q666 [PubMed: 36606703]
4. Yang F. et al. Palette of Rechargeable Mechanoluminescent Fluids Produced by a Biomineral-Inspired Suppressed Dissolution Approach. J. Am. Chem. Soc 144, 18406–18418 (2022): 10.1021/iacs.2cQ6724 [PubMed: 36190898]
5. Yang F. et al. A biomineral-inspired approach of synthesizing colloidal persistent phosphors as a multicolor, intravital light source. Sci. Adv 8, eabo6743 (2022): DOI: 10.1126/sciadv.abo6743 [PubMed: 35905189]

References

1. Prominski A. et al. Porosity-based heterojunctions enable leadless optoelectronic modulation of tissues. Nat. Mater 21, 647–655 (2022). [PubMed: 35618824]
2. Tian B. Nongenetic neural control with light. Science 365, 457 (2019). [PubMed: 31371607]
3. Xu C. et al. Nanoparticles with ultrasound-induced afterglow luminescence for tumour-specific theranostics. Nat Biomed Eng (2022) doi:10.1038/s41551-022-00978-z.
4. Sebesta C. et al. Subsecond multichannel magnetic control of select neural circuits in freely moving flies. Nat. Mater 21, 951–958 (2022). [PubMed: 35761060]

5. Chen JC et al. A wireless millimetric magnetoelectric implant for the endovascular stimulation of peripheral nerves. Nat Biomed Eng 6, 706–716 (2022). [PubMed: 35361934]
6. Jiang S. et al. Spatially expandable fiber-based probes as a multifunctional deep brain interface. Nat. Commun 11, 6115 (2020). [PubMed: 33257708]
7. Yun SH & Kwok SJJ Light in diagnosis, therapy and surgery. Nature Biomedical Engineering vol. 1 Preprint at 10.1038/s41551-016-0008 (2017).
8. Jiang S, Wu X, Rommelfanger NJ, Ou Z & Hong G Shedding light on neurons: optical approaches for neuromodulation. Natl Sci Rev 9, nwac007 (2022). [PubMed: 36196122]
9. Hong G, Antaris AL & Dai H Near-infrared fluorophores for biomedical imaging. Nature Biomedical Engineering vol. 1 Preprint at 10.1038/s41551-016-0010 (2017).
10. Zhang F. et al. Optogenetic interrogation of neural circuits: technology for probing mammalian brain structures. Nat. Protoc 5, 439–456 (2010). [PubMed: 20203662]
11. Kim P. et al. In vivo wide-area cellular imaging by side-view endomicroscopy. Nat. Methods 7, 303–305 (2010). [PubMed: 20228814]
12. Keahey P, Ramalingam P, Schmeler K & Richards-Kortum RR Differential structured illumination microendoscopy for in vivo imaging of molecular contrast agents. Proc. Natl. Acad. Sci. U. S. A 113, 10769–10773 (2016). [PubMed: 27621464]
13. Yang Y. et al. Preparation and use of wireless reprogrammable multilateral optogenetic devices for behavioral neuroscience. Nat. Protoc 17, 1073–1096 (2022). [PubMed: 35173306]
14. Ausra J et al. Wireless, battery-free, subdermally implantable platforms for transcranial and long-range optogenetics in freely moving animals. Proc. Natl. Acad. Sci. U. S. A 118, (2021).
15. Montgomery KL et al. Wirelessly powered, fully internal optogenetics for brain, spinal and peripheral circuits in mice. Nat. Methods 12, 969–974 (2015). [PubMed: 26280330]
16. Chen S et al. Near-infrared deep brain stimulation via upconversion nanoparticle-mediated optogenetics. Science 359, 679–684 (2018). [PubMed: 29439241]
17. Wu X et al. Tether-free photothermal deep-brain stimulation in freely behaving mice via wide-field illumination in the near-infrared-II window. Nat Biomed Eng 6, 754–770 (2022). [PubMed: 35314800]
18. Ruan H et al. Deep tissue optical focusing and optogenetic modulation with time-reversed ultrasonically encoded light. Sci Adv 3, eaao5520 (2017). [PubMed: 29226248]
19. Hong G Seeing the sound. Science 369, 638 (2020). [PubMed: 32764064]
20. Wu X et al. Sono-optogenetics facilitated by a circulation-delivered rechargeable light source for minimally invasive optogenetics. Proc. Natl. Acad. Sci. U. S. A 116, 26332–26342 (2019). [PubMed: 31811026]
21. Wang W et al. Ultrasound-Triggered In Situ Photon Emission for Noninvasive Optogenetics. J. Am. Chem. Soc 145, 1097–1107 (2023). [PubMed: 36606703]
22. Yang F et al. Palette of Rechargeable Mechanoluminescent Fluids Produced by a Biomineral-Inspired Suppressed Dissolution Approach. J. Am. Chem. Soc 144, 18406–18418 (2022). [PubMed: 36190898]
23. Yang F et al. A biomineral-inspired approach of synthesizing colloidal persistent phosphors as a multicolor, intravital light source. Sci Adv 8, eabo6743 (2022). [PubMed: 35905189]
24. Yang F et al. Principles and applications of sono-optogenetics. Advanced Drug Delivery Reviews vol. 194 114711 Preprint at 10.1016/j.addr.2023.114711 (2023). [PubMed: 36708773]
25. Zhou XX et al. A Single-Chain Photoswitchable CRISPR-Cas9 Architecture for Light-Inducible Gene Editing and Transcription. ACS Chem. Biol 13, 443–448 (2018). [PubMed: 28938067]
26. Li X, Lovell JF, Yoon J & Chen X Clinical development and potential of photothermal and photodynamic therapies for cancer. Nature Reviews Clinical Oncology vol. 17 657–674 Preprint at 10.1038/s41571-020-0410-2 (2020).
27. Kim T-I et al. Injectable, cellular-scale optoelectronics with applications for wireless optogenetics. Science 340, 211–216 (2013). [PubMed: 23580530]
28. Salatino JW, Ludwig KA, Kozai TDY & Purcell EK Glial responses to implanted electrodes in the brain. Nat Biomed Eng 1, 862–877 (2017). [PubMed: 30505625]

29. Shahriari D, Rosenfeld D & Anikeeva P Emerging Frontier of Peripheral Nerve and Organ Interfaces. Neuron 108, 270–285 (2020). [PubMed: 33120023]
30. Hibberd TJ et al. Optogenetic Induction of Colonic Motility in Mice. Gastroenterology 155, 514–528.e6 (2018). [PubMed: 29782847]
31. Xian Q et al. Modulation of deep neural circuits with sonogenetics. Proc. Natl. Acad. Sci. U. S. A 120, e2220575120 (2023). [PubMed: 37216521]
32. Airan RD & Butts Pauly K Hearing out Ultrasound Neuromodulation. Neuron vol. 98 875–877 (2018). [PubMed: 29879389]
33. Sato T, Shapiro MG & Tsao DY Ultrasonic Neuromodulation Causes Widespread Cortical Activation via an Indirect Auditory Mechanism. Neuron 98, 1031–1041.e5 (2018). [PubMed: 29804920]
34. Guo H et al. Ultrasound Produces Extensive Brain Activation via a Cochlear Pathway. Neuron vol. 98 1020–1030.e4 Preprint at 10.1016/j.neuron.2018.04.036 (2018). [PubMed: 29804919]
35. Mohammadjavadi M et al. Elimination of peripheral auditory pathway activation does not affect motor responses from ultrasound neuromodulation. Brain Stimul. 12, 901–910 (2019). [PubMed: 30880027]
36. Ye PP, Brown JR & Pauly KB Frequency Dependence of Ultrasound Neurostimulation in the Mouse Brain. Ultrasound Med. Biol 42, 1512–1530 (2016). [PubMed: 27090861]
37. Yang J-M et al. Simultaneous functional photoacoustic and ultrasonic endoscopy of internal organs in vivo. Nat. Med 18, 1297–1302 (2012). [PubMed: 22797808]
38. Arenkiel BR et al. In vivo light-induced activation of neural circuitry in transgenic mice expressing channelrhodopsin-2. Neuron 54, 205–218 (2007). [PubMed: 17442243]
39. Kefauver JM, Ward AB & Patapoutian A Discoveries in structure and physiology of mechanically activated ion channels. Nature 587, 567–576 (2020). [PubMed: 33239794]
40. Oh S-J et al. Ultrasonic Neuromodulation via Astrocytic TRPA1. Curr. Biol 29, 3386–3401.e8 (2019). [PubMed: 31588000]
41. Hu Z, Chen S, Yang Y, Gong Y & Chen H An Affordable and Easy-to-Use Focused Ultrasound Device for Noninvasive and High Precision Drug Delivery to the Mouse Brain. IEEE Trans. Biomed. Eng 69, 2723–2732 (2022). [PubMed: 35157574]

KEY POINTS

- The procedures cover the synthesis and characterization of mechanoluminescent nanotransducers covering the entire visible spectrum; their characterization in response to ultrasound in tissue-mimicking phantoms and in artificial circulatory systems and a demonstration of their use in a mouse behavioral assay and in an immunohistochemical assay of c-fos.
- Alternative deep-tissue light delivery approaches include implanted light sources based on optical fibers or μ-LEDs, intracranially-injected light sources based on upconversion nanoparticles, and wavefront shaping methods based on spatial light modulators

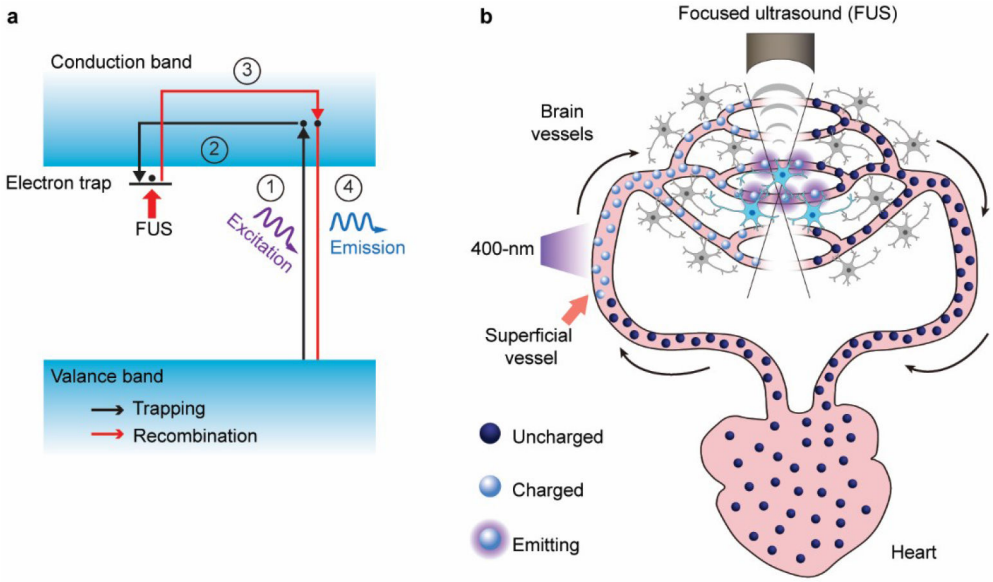

Fig. 1 | Principles of deLight.

a, Mechanism of light emission from charged MLNTs upon FUS stimulation. **b**, A schematic illustration of the charging (photoexcitation) and discharging (photoemission) processes of MLNTs during circulation. Adapted with permission from Ref. 20.

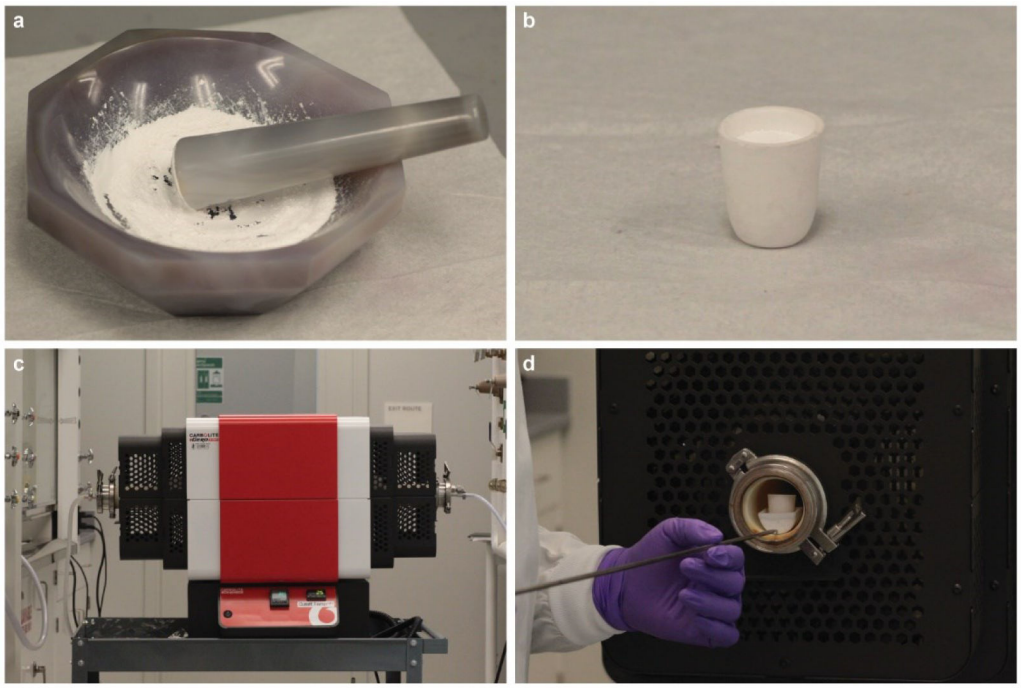

Fig. 2 | Synthesis of bulk mechanoluminescent materials via solid-state reactions.
a, Grind the reagents with an agate mortar and a pestle. **b,** Transfer the ground reagents into an alumina crucible. **c,** The tube furnace used for solid-state reactions. **d,** Place the combustion boat in the tube furnace with a hook.

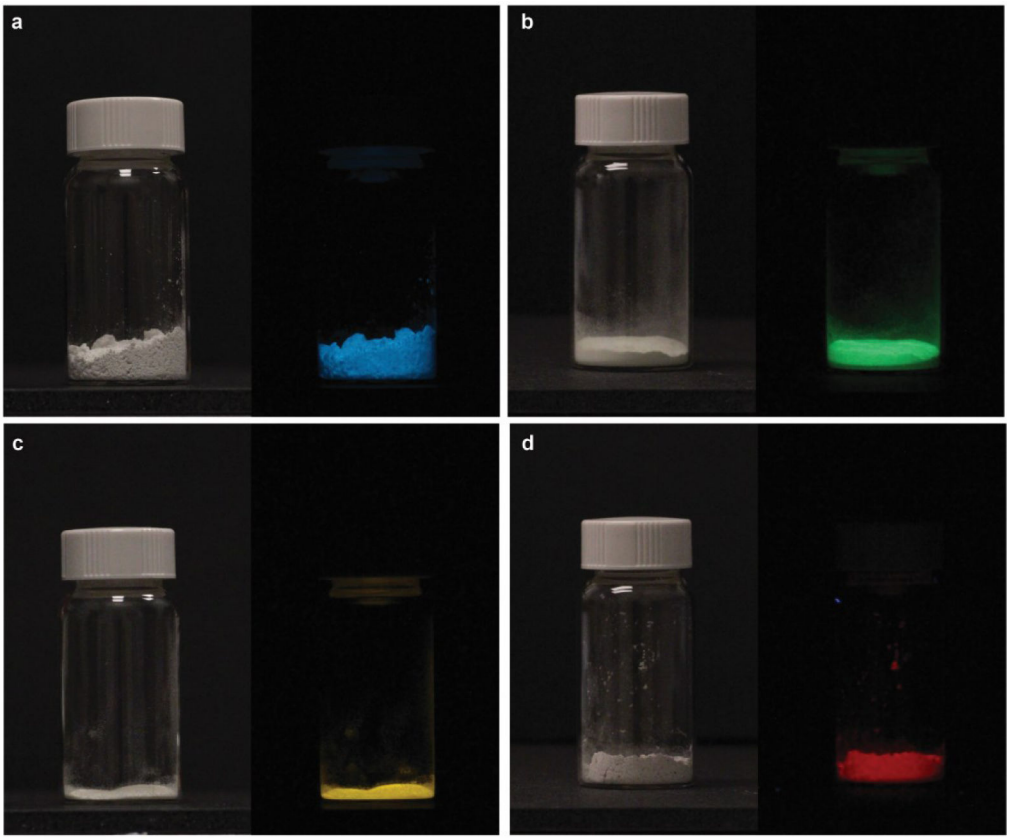

Fig. 3 |. Bright-field (left) and afterglow (right) images of as-synthesized mechanoluminescent materials:

a, $Sr_2MgSi_2O_7$:Eu,Dy; **b,** ZnS:Cu,Al; **c,** ZnS:Mn; and **d,** $CaTiO_3$:Pr.

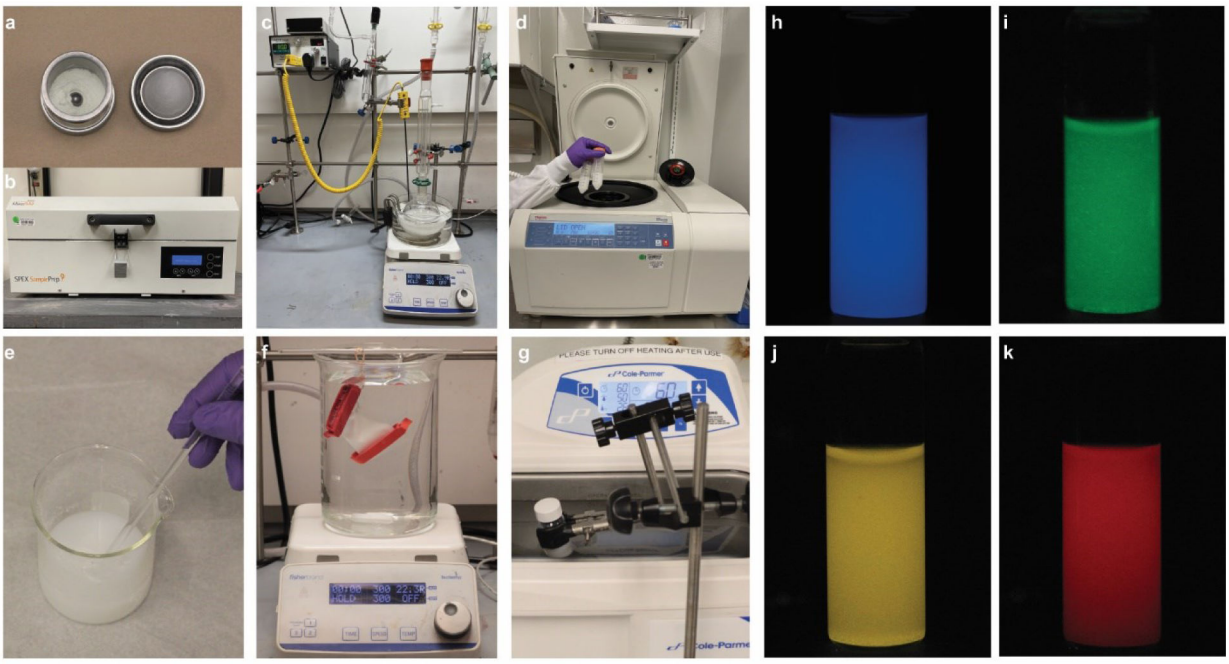

Fig. 4 | Synthesis of biocompatible MLNTs.

a-b, Ball-milling process of the bulk mechanoluminescent material: **a**, A tungsten carbide grinding vial loaded with the as-synthesized bulk mechanoluminescent material and a tungsten carbide grinding ball; **b**, The ball-mill machine used in this protocol. **c**, The setup used for the biomineral-inspired suppressed dissolution approach. **d**, Colloidal solutions of MLNTs collected after the first centrifuge process. **e**, Addition and dissolution of NaCl in the colloidal solution to facilitate its precipitation for purification. **f**, Dialysis of the colloid. **g**, Sonication of the colloid to facilitate its reaction with NaOH. **h-k**, Afterglow luminescent images of MLNT colloidal solutions of **h**, $Sr_2MgSi_2O_7$:Eu,Dy; **i**, ZnS:Cu,Al; **j**, ZnS:Mn; and **k**, $CaTiO_3$:Pr. Reproduced with permission from Ref. 22.

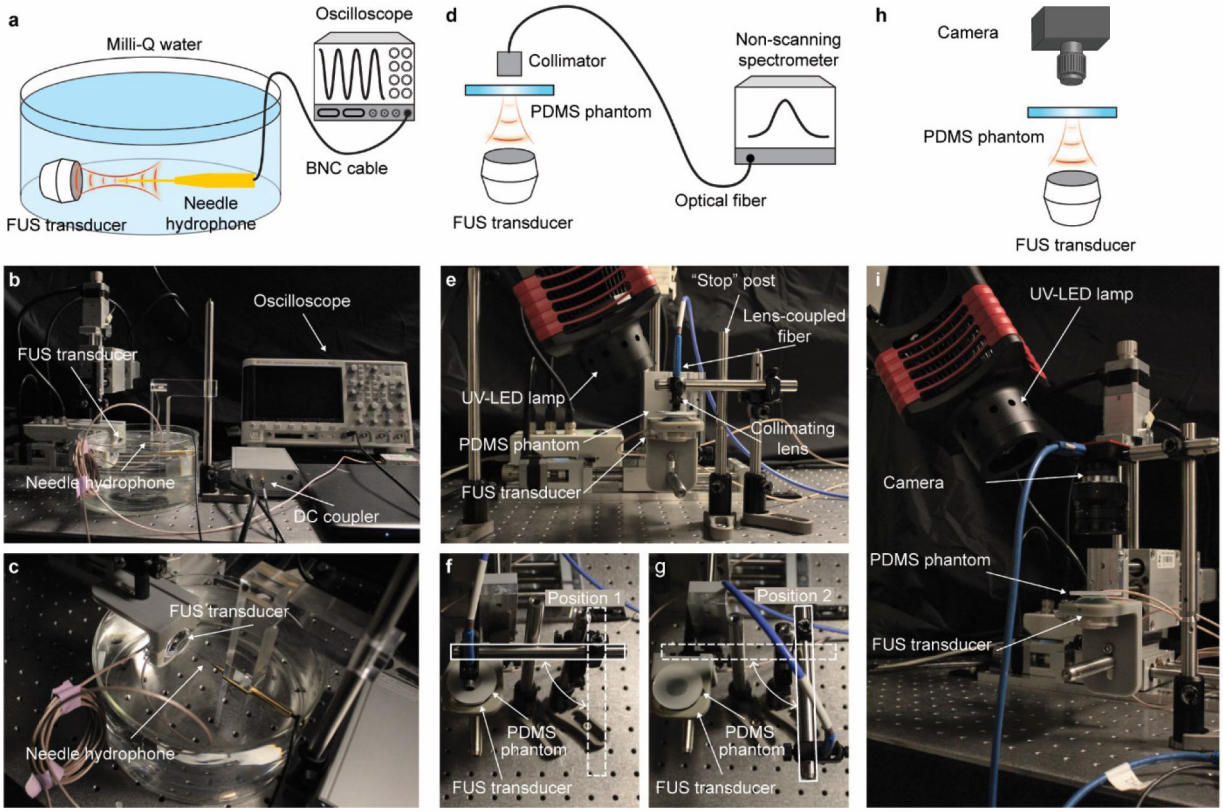

Fig. 5 |. Characterizations of MLNTs in a tissue-mimicking phantom.

a, A schematic illustration of the FUS calibration process. **b**, Experimental setup of **a**. **c**, A zoom-in photograph showing the alignment of the transducer and the needle hydrophone. **d**, A schematic illustration of the setup for measuring the mechanoluminescence spectrum of the PDMS phantom under FUS. Adapted with permission from Ref. 22. **e**, Experimental setup of **d**. **f**, A top view of Position 1, where the lens-coupled optical fiber is aligned with the center of the transducer in the z-direction. **g**, A top view of Position 2, where the lens-coupled optical fiber is away from the PDMS phantom. **h**, A schematic illustration for visualizing mechanoluminescence emission from the PDMS phantom under FUS with a camera. **i,** Experimental setup of **h**.

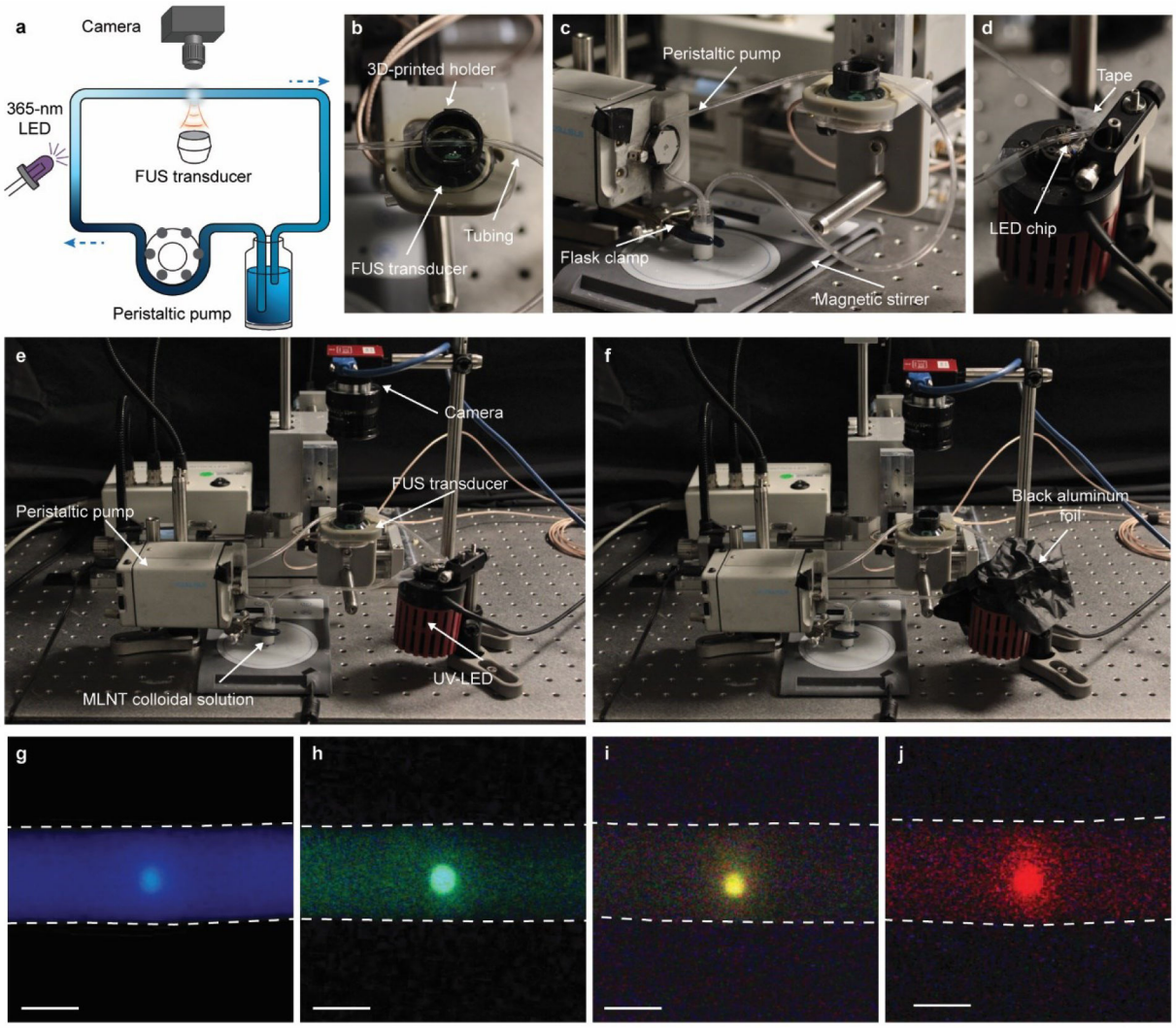

Fig. 6 | Characterizations of MLNTs in an artificial circulatory system.

a, A schematic illustration of the artificial circulatory system. Reproduced with permission from Ref. 22. **b**, A 3D-printed holder that can be tightly mounted on the transducer where the inserted tubing lies at the focus of the FUS transducer. **c**, The construction of the artificial circulatory system. **d**, The UV-LED with a segment of the tubing fixed on top of the LED chip. **e**, The complete setup for the characterizations of MLNTs in the artificial circulatory system. **f**, Black aluminum foil used for blocking stray light leaking from the UV-LED during image acquisition. **g-j**, Representative images of FUS-induced emission from the tubing filled with the MLNT colloidal solution of **g**, $Sr_2MgSi_2O_7$:Eu,Dy; **h**, ZnS:Cu,Al; **i**, ZnS:Mn; and **j**, $CaTiO_3$:Pr. All scale bars represent 1 mm. Reproduced with permission from Ref. 22.

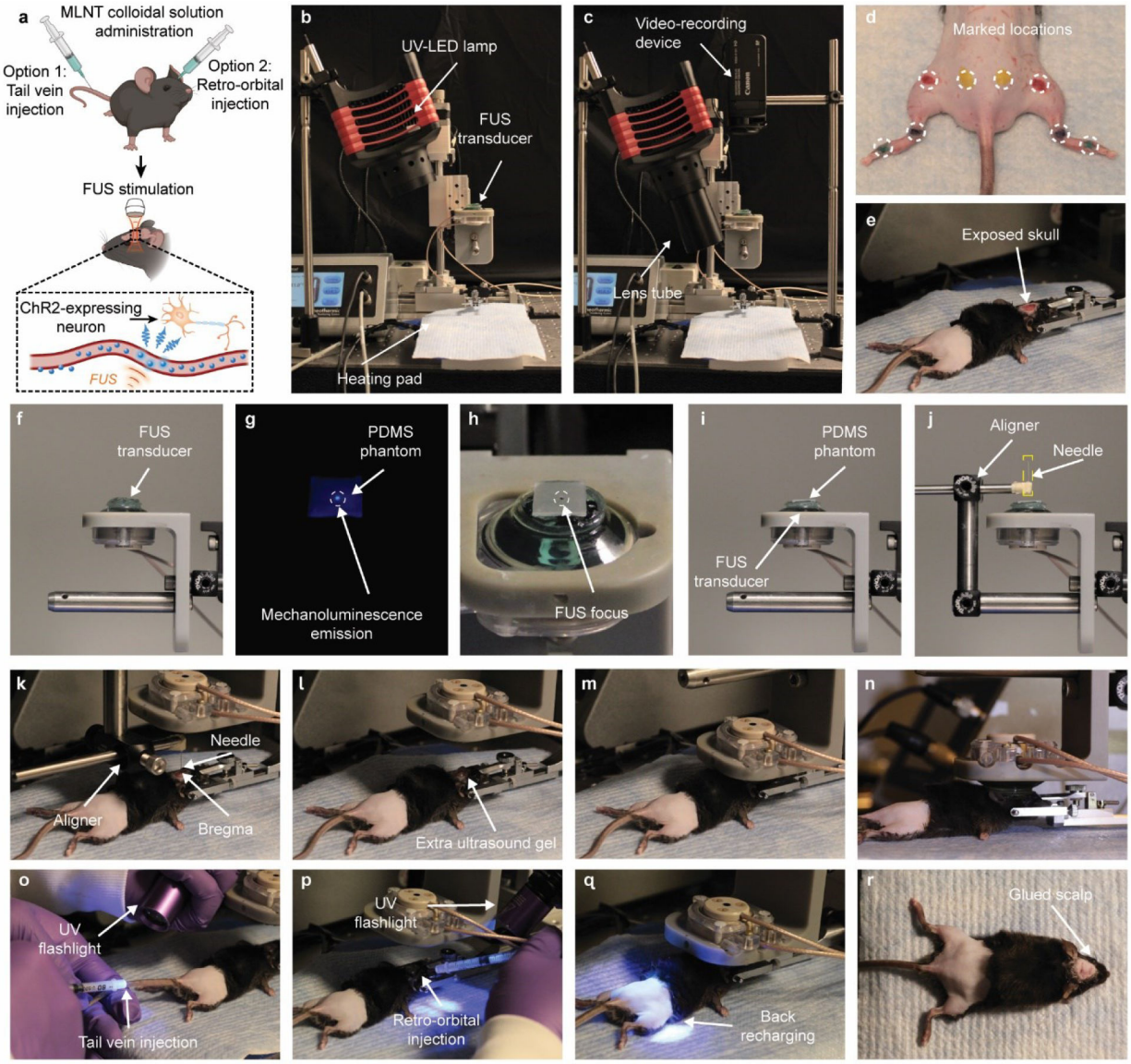

Fig. 7 | Application of deLight *in vivo*.

a, A schematic illustration of the application of delight *in vivo*. Adapted with permission from Ref. 22. **b**, The setup for applying deLight in optogenetic neuromodulation followed by c-fos immunostaining. **c**, The setup for applying deLight in optogenetic neuromodulation with simultaneous behavioral monitoring. **d**, Photograph showing the marked locations on the mouse's back. **e**, A head-mounted animal with its skull exposed and part of the fur removed. **f**, A side view of the FUS transducer. **g**, PDMS phantom showing bright emission at the focus of applied ultrasound. **h**, A marked dot on the PMDS phantom indicating the focus of the FUS transducer. **i**, A side view of the transducer with the PDMS phantom. **j**, Align the needle of the "L" shaped aligner with the marked dot on the PDMS phantom in the *z*-direction. **k**, Rotate the transducer with the aligner and align the needle with the marked bregma of the mouse skull. **l**, Remove the aligner and the PDMS phantom, and apply extra ultrasound gel. **m**, Move the transducer to the desired brain coordinates and lower

the transducer. **n**, A side view of the transducer and the mouse head showing their relative positions. **o**, Tail-vein injection of the loaded MLNT solution charged by a UV flashlight. **p**, Retro-orbital injection of the loaded MLNT solution charged by a UV flashlight. **q**, After injection of the MLNT solution, start FUS pulses and UV recharging on the back. **r**, Glue the scalp back at the end of the deLight stimulation session.

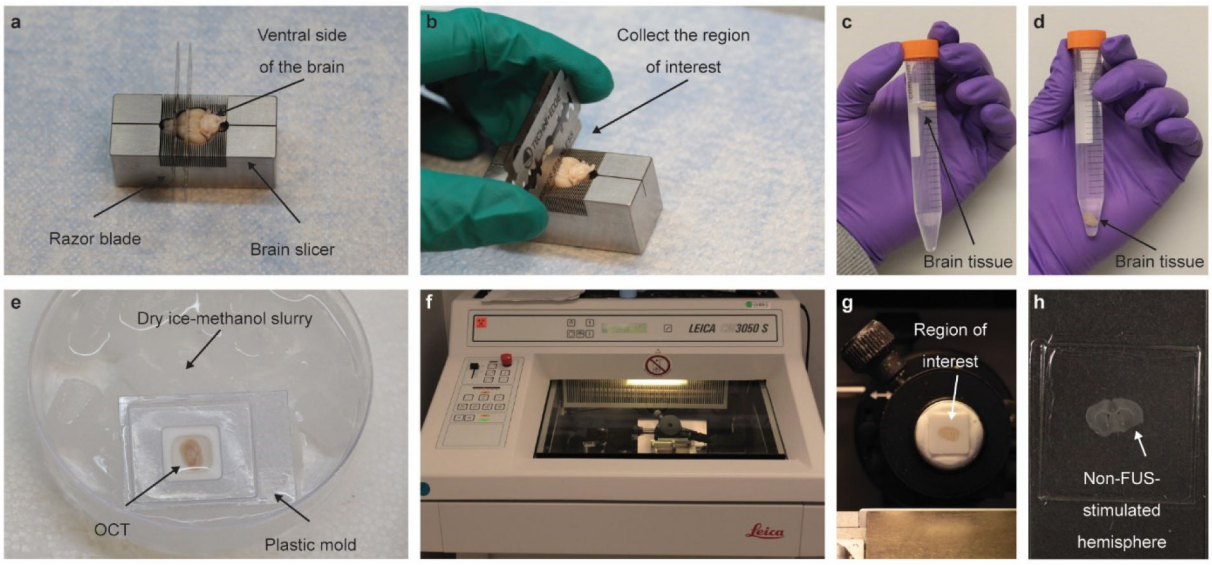

Fig. 8 |. Dissection and staining of brain sections to evaluate the efficacy of deLight.

a, Determine the region of interest from the ventral side of the brain. **b**, Collect tissue blocks with razor blades. **c**, A brain tissue block floating in the sucrose solution upon immersion. **d**, A brain tissue block sinking to the bottom of the sucrose solution. **e**, Frozen embedding process of the brain tissue block in the O.C.T. compound. **f**, Cryostat used in this protocol. **g**, Collection of brain sections of interest. **h**, Mounted a brain section on a glass slide with the cut marking the hemisphere stimulated with deLight.

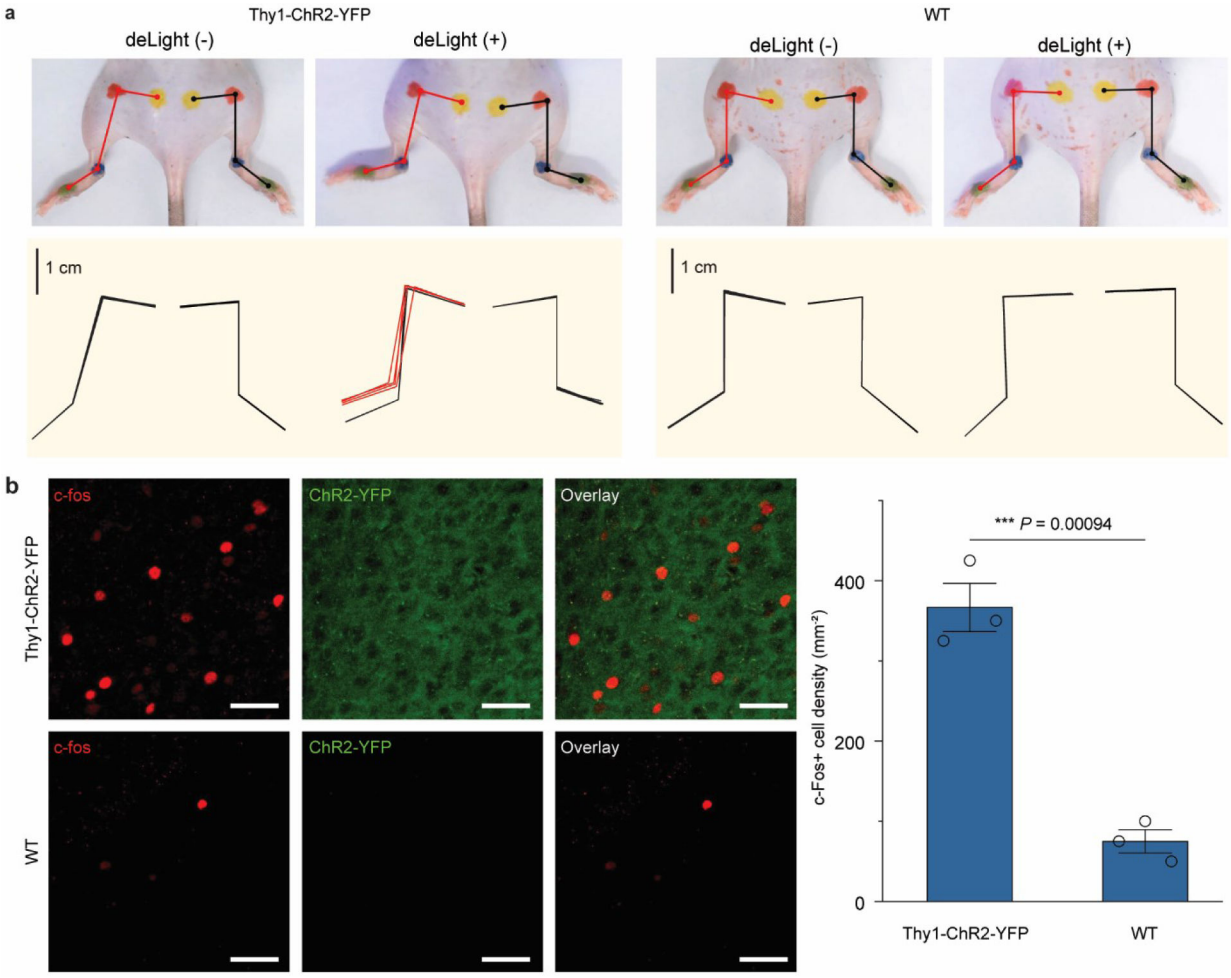

Fig. 9 | Representative results of *in vivo* sono-optogenetic neuromodulation with deLight.
a, Tracking of mouse limb movements produced by optogenetic neuromodulation via deLight in the brain. Reproduced with permission from Ref. 20. **b**, Immunostaining of c-fos, an immediate early gene that labels recent neuron activity, in mouse brain sections after neuromodulation with deLight. All scale bars represent 40 μm. Reproduced with permission from Ref. 22.

Table 1

Synthesis conditions and peak wavelengths of mechanoluminescent materials

Mechanoluminescent material	Reagents	Temperature (T) program	Environment	Peak wavelength
$Sr_2MgSi_2O_7$:Eu,Dy	$SrCO_3$ (2332.56 mg; 15.8 mmol), SiO_2 (961.28 mg; 16 mmol), Eu_2O_3 (8.4 mg, 0.024 mmol), Dy_2O_3 (29.84 mg; 0.08 mmol),$(MgCO_3)_4{\cdot}Mg(OH)_2{\cdot}5H_2O$ (777.04 mg; 1.6 mmol), and H_3BO_3 (29.66 mg; 0.48 mmol)	Increase T to 800 °C at a ramp rate of 10 °C/min; increase T from 800 °C to 1050 °C at a ramp rate of 5 °C/min; maintain at 1050 °C for 2 h; cool down to room temperature.	5% H_2 in Ar	470 nm
ZnS:Cu,Al	ZnS (1960 mg; 20 mmol), Al_2O_3 (6 mg; 0.06 mmol), H_3BO_3 (12 mg; 0.19 mmol), and 20 μl of the copper stock solution	Increase T to 800 °C at a ramp rate of 10 °C/min; increase T from 800 °C to 1100 °C at a ramp rate of 5 °C/min; maintain at 1100 °C for 2 h; cool down to room temperature.	5% H_2 in Ar	534 nm
ZnS:Mn	ZnS (1960 mg; 20 mmol), $MnCO_3$ (2.3 mg; 0.02 mmol), and H_3BO_3 (12 mg; 0.19 mmol)	Increase T to 800 °C at a ramp rate of 10 °C/min; increase T from 800 °C to 1100 °C at a ramp rate of 5 °C/min; maintain at 1100 °C for 2 h; cool down to room temperature.	5% H_2 in Ar	578 nm
$CaTiO_3$:Pr	$CaCO_3$ (1000 mg; 10 mmol), TiO_2 (800 mg; 10 mmol), and Pr_2O_3 (49 mg; 0.15 mmol)	Increase T to 800 °C at a ramp rate of 10 °C/min; increase T from 800 °C to 1300 °C at a ramp rate of 5 °C/min; maintain at 1300 °C for 2 h; cool down to room temperature.	Air	614 nm

Table 2

Antibodies

Primary antibody			Secondary antibody		
Name	**Dilution**	**Company name and cat. no.**	**Name**	**Dilution**	**Company name and cat. no.**
Recombinant Anti-c-Fos antibody (rabbit monoclonal)	1:1000	Abcam, cat. no. ab222699	Donkey anti-Rabbit IgG (H+L) Highly Cross-Adsorbed Secondary Antibody, Alexa Fluor™ 594	1:500	Thermo Fisher Scientific, cat. no. A-21207

Table 3.

Troubleshooting table

Procedure	Step	Problem	Possible reason	Possible solution
1	11	As-synthesized $Sr_2MgSi_2O_7$:Eu,Dy, ZnS:Cu,Al, and ZnS:Mn bulk mechanoluminescent materials exhibit weak afterglow.	The ends of the tube furnace are not tightly sealed.	Check the seal of the tube furnace with soapy water and re-seal the tube again.
1	37	There are insufficient MLNTs to make 20 mL solution at a concentration of at least 6 mg/mL.	The yield of MLNTs synthesized from the biomineral-inspired suppressed dissolution approach in Procedure 1, Steps 18-21 is low. Possible causes of this low yield include a reaction temperature lower than 80°C, incomplete reflux of solvent condensation in the condenser, and excessive ion strengths due to an incorrect buffer concentration.	1) Maintain the reaction temperature at 80°C with minimal fluctuation throughout the suppressed dissolution procedure; 2) Ensure minimal loss of solvent due to evaporation during the synthesis of MLNTs; 3) Ensure a constant concentration of the sodium citrate buffer at 0.08 mol/L throughout the reaction.
1	44	Flocculations appear in the vial after sonication.	mPEG-silane is hydrolyzed.	Wash MLNTs thoroughly with DMF to remove residual water.
1	48	Colloidal solutions of MLNTs appear dim in the dark.	The MLNT colloidal solution may have stayed too long in the dark without further recharging.	Charge the MLNT colloidal solution and examine its afterglow in the dark immediately after recharging.
2	7	PDMS phantom shows some porous structure after curing.	Air bubbles may have not been thoroughly removed in the vacuum desiccator.	Increase the vacuuming time of the mixture inside the vacuum desiccator.
2	22	The peak-to-peak voltage signal is too low or noisy.	The alignment between the needle hydrophone and FUS transducer is not optimized.	Check the alignment and the orientation between the needle hydrophone and FUS transducer to obtain the highest voltage.
2	45	The intensity of the mechanoluminescence spectrum is too low, or the spectrum is too noisy.	The PDMS phantom is misaligned from the ultrasound focus, or the light emission spot is misaligned from the lens-coupled fiber.	1) Make sure the focus of the FUS transducer is positioned within the PDMS phantom according to Extended Data Fig. 3. 2) Make sure there are no air bubbles in the ultrasound gel between the transducer and the PDMS phantom. 3) Adjust the position of the lens-coupled fiber to make sure it is vertically aligned with the ultrasound focus for efficient light collection.
2	63	No image file is saved.	The hardware (i.e., FUS system and UV-LED lamp) are not connected to the correct ports of the I/O device.	Adjust the connection between the hardware and the I/O device and make sure the analog output ports of the I/O device are connected as described in the protocol.
3	23	No emission is observed.	1) MLNT colloidal solution is not flowing inside the tubing. 2) The charging segment of the tubing falls off the LED chip.	Check the ends of the tubing in the glass vial to ensure a continuous flow of the colloidal solution. Check the tubing on the UV-LED chip to ensure continuous recharging of the colloidal solution.
4	19	No bright spot is observed in the PDMS phantom under FUS.	There may be air bubbles in the ultrasound gel between the FUS transducer and the PDMS phantom to hinder ultrasound transmission.	Check the interface between the FUS transducer and the PDMS phantom and remove air bubbles. Add additional ultrasound gel if needed.
4	39	The animal responds to toe pinch.	The animal is gradually waking up. from initial dosage of anesthetic drug.	Additional dose of the anesthetic drug may be needed until the animal shows no responses to a toe pinch. In our experience, a supplemental anesthetic (25% of the initial dose) can be given at ca. 70 min after deLight application.

Procedure	Step	Problem	Possible reason	Possible solution
4	73	The image is too dim.	The imaging setting is not optimized.	Adjust the laser intensity, pinhole size, and gain to improve the image quality.
4	74	No detectable c-fos expression is evident in the brain sections within the hemisphere where FUS was applied.	The FUS transducer may have been misaligned with respect to the mouse bregma, thus yielding off-target stimulation in the brain.	Expand the search of positive c-fos signals in neighboring coronal sections. This expanded search can be done by staining multiple brain sections, extending their range to include AP coordinates ±1 mm from the original AP coordinate. The sections should be taken at intervals of 200 μm, and the process should continue until positive c-fos signals are identified.